NAVAL POSTGRADUATE SCHOOL
Monterey, California

THESIS

TIME AND SPACE RESOLUTION AND MIXED LAYER MODEL ACCURACY

by

David Michael Hone

March, 1997

Co-Advisors: R.W. Garwood, Jr.
A.A. Guest

Approved for public release; distribution is unlimited.

REPORT DOCUMENTATION PAGE

Form Approved OMB No. 0704-0188

1. AGENCY USE ONLY *(Leave blank)*	2. REPORT DATE March 1997	3. REPORT TYPE AND DATES COVERED Master's Thesis

4. TITLE AND SUBTITLE Time and Space Resolution and Mixed Layer Model Accuracy (Unclassified)

5. FUNDING NUMBERS

6. AUTHOR(S) David Michael Hone

7. PERFORMING ORGANIZATION NAME(S) AND ADDRESS(ES)
Naval Postgraduate School
Monterey CA 93943-5000

8. PERFORMING ORGANIZATION REPORT NUMBER

9. SPONSORING/MONITORING AGENCY NAME(S) AND ADDRESS(ES)

10. SPONSORING/MONITORING AGENCY REPORT NUMBER

11. SUPPLEMENTARY NOTES The views expressed in this thesis are those of the author and do not reflect the official policy or position of the Department of Defense or the U.S. Government.

12a. DISTRIBUTION/AVAILABILITY STATEMENT
Approved for public release; distribution is unlimited.

12b. DISTRIBUTION CODE

13. ABSTRACT *(maximum 200 words)*

The oceanic turbulent boundary layer is a critical region to understand for oceanic and atmospheric prediction. This thesis answers two fundamental questions: (i) what is the response of the ocean mixed layer system to transient forcing at the air sea surface? (ii) what is the necessary time and space resolution in an ocean mixed layer model to resolve important transient responses?

Beginning with replication of de Szoeke and Rhines' (1976) work, additional physical processes were added to include more realistic viscous dissipation and anisotropy in the three-dimensional turbulent kinetic energy (TKE) budget. These refinements resulted in modification of de Szoeke and Rhines' findings. Firstly, TKE unsteadiness is important for a minimum of 10^5 seconds. Secondly, viscous dissipation should not be approximated as simply proportional to shear production. Thirdly, entrainment shear production remains significant for a minimum of one pendulum-day.

The required temporal model resolution is dependent on the phenomena to be studied. This study focused on the diurnal, synoptic, and annual cycles, which the one-hour time step of the Naval Postgraduate School model adequately resolves. The study of spatial resolution showed unexpectedly that model skill was comparable for 1 m, 10 m and even 20 m vertical grid spacing.

14. SUBJECT TERMS Ocean mixed layer, numerical modeling, turbulent boundary layer, model resolution.			15. NUMBER OF PAGES 68
			16. PRICE CODE
17. SECURITY CLASSIFICATION OF REPORT Unclassified	18. SECURITY CLASSIFICATION OF THIS PAGE Unclassified	19. SECURITY CLASSIFICATION OF ABSTRACT Unclassified	20. LIMITATION OF ABSTRACT UL

NSN 7540-01-280-5500

Standard Form 298 (Rev. 2-89)
Prescribed by ANSI Std. 239-18 298-102

Approved for public release; distribution is unlimited.

TIME AND SPACE RESOLUTION AND MIXED LAYER MODEL ACCURACY

David M. Hone
Lieutenant, United States Navy
B.S., Florida Institute of Technology, 1988

Submitted in partial fulfillment
of the requirements for the degree of

MASTER OF SCIENCE IN METEOROLOGY AND PHYSICAL OCEANOGRAPHY

from the

NAVAL POSTGRADUATE SCHOOL
March 1997

ABSTRACT

The oceanic turbulent boundary layer is a critical region to understand for oceanic and atmospheric prediction. This thesis answers two fundamental questions:(i) what is the response of the ocean mixed layer system to transient forcing at the air sea surface? (ii) what is the necessary time and space resolution in an ocean mixed layer model to resolve important transient responses?

Beginning with replication of de Szoeke and Rhines' (1976) work, additional physical processes were added to include more realistic viscous dissipation and anisotropy in the three-dimensional turbulent kinetic energy (TKE) budget. These refinements resulted in modification of de Szoeke and Rhines' findings. Firstly, TKE unsteadiness is important for a minimum of 10^5 seconds. Secondly, viscous dissipation should not be approximated as simply proportional to shear production. Thirdly, entrainment shear production remains significant for a minimum of one pendulum-day.

The required temporal model resolution is dependent on the phenomena to be studied. This study focused on the diurnal, synoptic, and annual cycles, which the one-hour time step of the Naval Postgraduate School model adequately resolves. The study of spatial resolution showed unexpectedly that model skill was comparable for 1 m, 10 m and even 20 m vertical grid spacing.

TABLE OF CONTENTS

ACKNOWLEDGEMENT

The author wants to thank Professor R. W. Garwood, Jr., Ms. A. A. Guest, and Mr. R. R. Harcourt for their guidance and patience during the work in performing this investigation.

The author wants to thank his wife, Anne, for her support during this educational endeavor.

I. INTRODUCTION

A. STATEMENT OF PROBLEM

The oceanic turbulent boundary layer or mixed layer is a critical region to understand when studying the atmosphere or ocean. The ocean is the primary source of moisture fluxed into the atmosphere, it is a significant source of heat fluxed into the atmosphere in many regions, and it is a moderator of atmospheric extremes. To accurately model the atmosphere or ocean, a realistic representation of the turbulent mixed layer is required. This thesis will address two fundamental questions:(i) what is the response of the ocean mixed layer system to transient forcing at the air sea surface?; (ii) what is the necessary time and space resolution in an ocean mixed layer model to resolve important transient responses? With the answers to these questions, air-ocean models will be a step closer to being realistically coupled. The result will be better predictions for both atmosphere and ocean.

B. METHOD

To accomplish this task, the work of de Szoeke and Rhines(1976) on wind driven mixing was replicated and then generalized to include surface heating and cooling. Their study in "Asymptotic regimes in mixed layer deepening" did not include physical processes associated with surface heat flux and anisotropy in the three-dimensional turbulent kinetic

energy(TKE) budget. With the addition of these critical physical processes, a more generalized study of the short time scale dependence of the mixed layer is possible. The study can be extended past the single day scale of de Szoeke and Rhines to the synoptic and annual time scales by shifting the method of solution from a Runge-Kutta numerical scheme to a FORTRAN-based gridded model. With the question of the minimum time scale resolved, new assumptions about mixed layer physics can be made which allow testing of spatial resolution. The Naval Postgraduate School(NPS) mixed layer model developed by Garwood (1977) was modified to test the effect on model skill of varying the vertical grid size using observed meteorological forcing and changing thermal structure at weather station Papa (50° N, 145° W).

II. THEORY, MODEL EQUATIONS, AND HYPOTHETICAL SOLUTIONS

A. AIR OCEAN COUPLING

The surface layer of the ocean responds to variations in wind stress, heat flux, moisture flux, and several other less significant factors. These factors have been examined in depth since Ekman's (1905)ground laying work.

B. REPLICATION OF DE SZOEKE AND RHINES (1976)

Initial modeling efforts for this study focused on reproducing and then building on the efforts of de Szoeke and Rhines (1976) as discussed in their paper "Asymptotic regimes in mixed-layer deepening." Niiler (1975) proposed the basic terms in the turbulent kinetic energy (TKE) equation studied by de Szoeke and Rhines:

$$\left(\frac{1}{2}N^2h^4 - u_*^4\frac{2}{f^2}(1-\cos ft) + C_0u_*^2h^2\right)\frac{dh}{dt} = 2m_0u_*^3h \qquad (1)$$

A B C D

Term A represents buoyant damping of TKE by entrainment, term B the shear production of TKE by entrainment, term C the spin up or storage of TKE, and term D the near-surface wind shear production of TKE minus viscous dissipation. Solar heating and surface heat flux were not included. Term C, the energy required to spin up the turbulence intensity, was not originally included by Niiler.

To mathematically define the components of the de Szoeke and Rhines model, the friction velocity or u_* must first be defined. The friction velocity (equation 2) is defined as the square root of the surface wind stress divided by the density of water.

$$u_* \equiv \sqrt{\frac{|\tau_{(0)}|}{\rho_o}} \qquad (2)$$

The Brunt-Vaisala or buoyancy frequency (N) is a measure of vertical stability. A value of $2\Pi/600$ sec^{-1} was used for initial model testing and in the hypothetical cases. The mixed layer depth is h. The Coriolis parameter (f) is defined as $2\Omega_z$ where Ω_z is the vertical component of planetary rotation. A nominal mid-latitude value of $1x10^{-4}$ sec^{-1} was used for f. In equation (1) C_0 and m_0 are dimensionless tuning coefficients for TKE spin up and net wind-shear production, respectively.

Buoyant damping of TKE by entrainment, term A, is the rate of decrease in turbulence due to the lifting upward of denser water originating below the mixed layer. The mixed layer is made more stable by the entrainment of colder denser water, with a commensurate increase in potential energy. Shear production due to entrainment, term B, is the conversion of mean kinetic energy to turbulent kinetic energy due to

shear across the base of the mixed layer. This term also results in a net gain in turbulence. Turbulence spin up, term C, is the TKE build up required before entrainment can occur. The wind stirring minus viscous dissipation, term D, represents the net input of energy into the mixed layer due to wind stress, τ_o, in equation (2). In de Szoeke and Rhines' model, viscous dissipation is also proportional to u_*^3 because surface heating and cooling are neglected as sources or sinks of TKE, and dissipation of TKE produced by entrainment shear production is not accounted for.

As a first step in demonstrating and understanding the physics that drive mixed layer deepening, de Szoeke and Rhines' results were replicated. Equation (1) was solved for the rate of mixed layer deepening, $W_e = \partial h/dt$. The result is referred to as the W_e equation, since the vertical change in h is due only to entrainment (no advection). The W_e equation was formulated as a MATLAB function, and solved using an intrinsic Runge-Kutta solution routine, ODE45. The MATLAB function is restricted to continuous functions. This restricts the model to deepening scenarios.

De Szoeke and Rhines simplified equation (1) by analyzing the time evolution of the mixed layer deepening process and determined which terms could be neglected during various time regimes. Analytic solutions to the equation were then

possible in those specific time regimes. Figure 2.1a is a reproduction of de Szoeke and Rhines results, and 2.1b depicts the results of a Runge-Kutta solution to equation (1).

De Szoeke and Rhines showed that initially shear production due to entrainment (term B) can be ignored, that turbulence spin up (term C) dominates, and that the mixed layer deepens at a rate proportional to u.t. This condition holds for the first 100 seconds of deepening. Next, surface wind stirring (term D) dominates. Deepening continues at a rate proportional to $t^{1/3}$. Term C begins to build in importance between 20 and 120 minutes, with the deepening rate proportional to $t^{1/2}$. Coriolis (term B) becomes a factor as the mean flow direction is turned away from the wind direction. After twelve hours, term B is no longer dominant. Deepening returns to a wind driven scenario and a rate proportional to $t^{1/3}$.

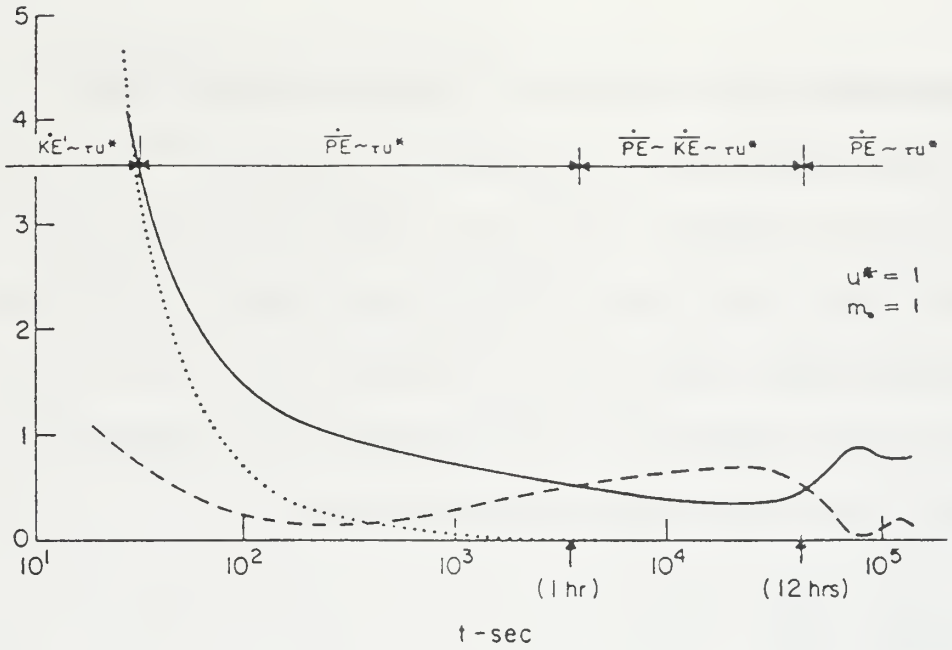

Figure 2.1a de Szoeke and Rhines solution. Solid curve: ratio D/A; dashed curve: ratio B/A; dotted curve: C/A .

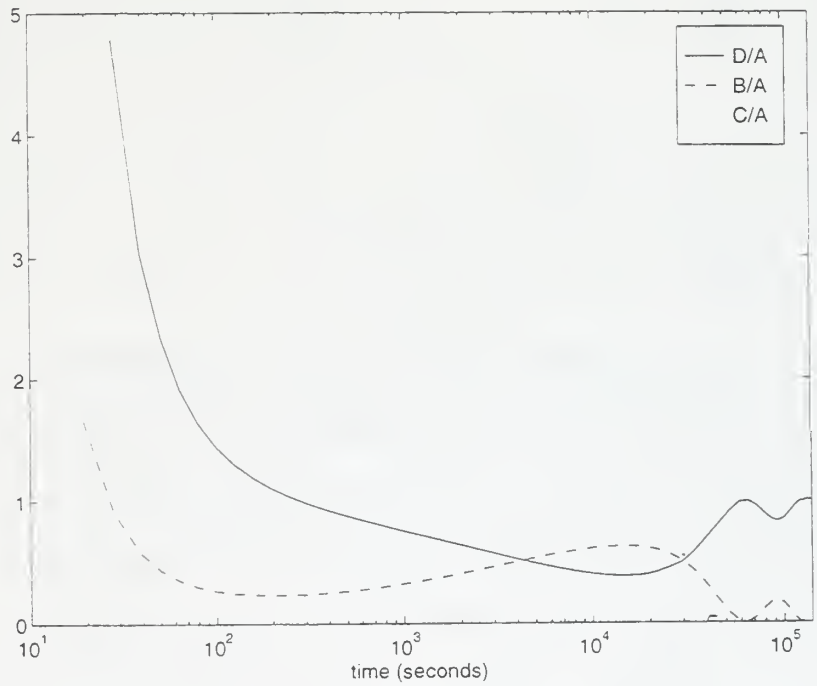

Figure 2.1b MATLAB ODE45 solution, replicating de Szoeke and Rhines.

C. IMPROVED MODEL PHYSICS TO INCLUDE EXPLICIT TKE

In the second model, the basic W_e equation is the same as in the first model, but three additional equations are included: the mixed layer temperature equation and the two horizontal mixed layer momentum equations. This allows the explicit calculation of the variables of temperature and velocity. The full set of equations are:

$$\frac{\partial T}{dt} = \frac{Q_o}{\rho C_p h} - \frac{\Delta T W_e}{h} \quad (3)$$

$$\frac{\partial u}{dt} = fv + \frac{\tau_x}{\rho h} - \frac{\Delta U W_e}{h} \quad (4)$$

$$\frac{\partial v}{dt} = -fu + \frac{\tau_y}{\rho h} - \frac{\Delta V W_e}{h} \quad (5)$$

$$\frac{\partial h}{dt} = \frac{2m_0 u_*^3 h^2 - \frac{\alpha g Q_0 h^3}{\rho c_p}}{\left(\frac{1}{2}N^2 h^4 - u_*^4 \frac{2}{f^2}(1-\cos ft) + C_0 u_*^2 h^2\right)} - W(z=-h) \quad (6)$$

In this more complete model with explicit momentum and heat equations, the ability to add steady state upwelling was included in the W_e equation. This model is identical to the original de Szoeke and Rhines model if the upwelling term, $W(z=-h)$, is set to zero, and if the net surface heat flux(Q_o) is neglected. However, when Q_o is nonzero in the second model, Q_o directly affects both the temperature equation (3) and the mixed layer depth equation (6), and it indirectly

affects momentum because of the W_e terms in equations (4) and (5). In the momentum equations, τ_x and τ_y are components of wind stress. ΔT is the change in temperature across the mixed layer interface (Figure 2.2); similarly, ΔU and ΔV are the changes in the velocity components across the interface.

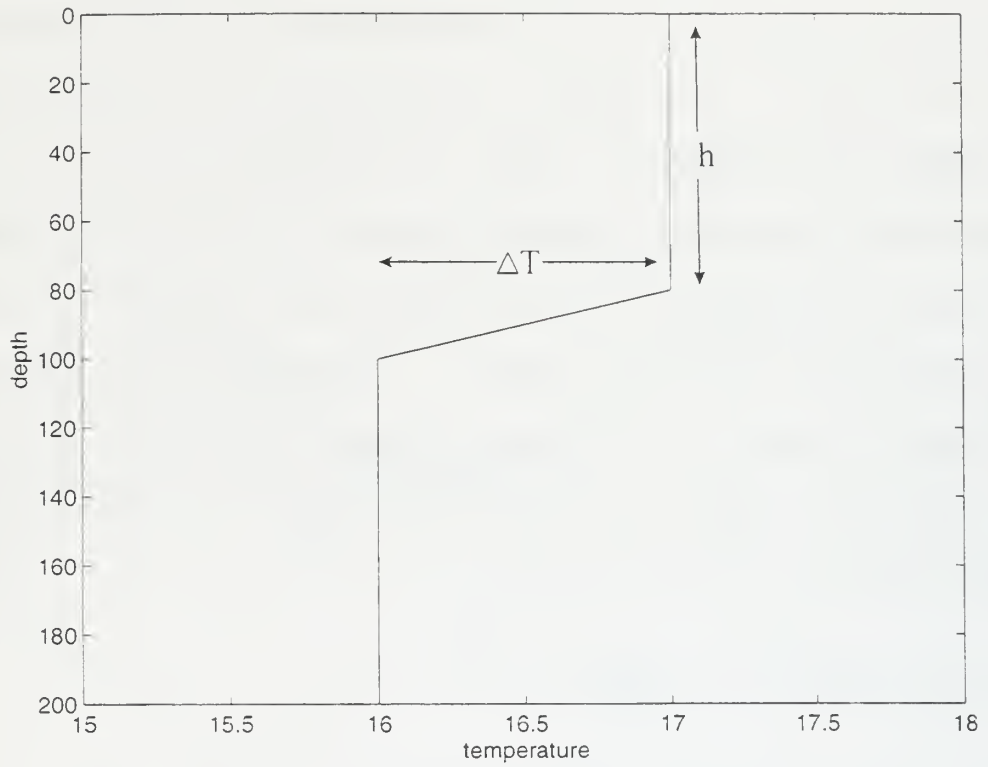

Figure 2.2 Hypothetical temperature profile.

The second model's solution for equation (6) was identical to de Szoeke and Rhines when Q_0 and $W(z=-h)$ were set to zero. The three additional equations allowed the explicit calculation of mixed layer temperature and velocity, but did not change the W_e solution. The model was initialized with both horizontal velocity components equal to zero and an SST

of 17° C with a linear temperature gradient with depth, having N = 2Π/600 seconds. A steady wind stress of 0.1 N/m^2 was applied in the τ_x direction. In 30 hours, the SST decreased to 16.3 C (Figure 2.3) as the cooler sub-mixed layer water was entrained. The horizontal velocities, u and v, respond to the steady state wind stress in the form of forced inertial motion. The period is dependent on latitude (2π/f) but a 90 degree phase shift between u and v is constant.

The third model is a MATLAB version of the NPS mixed layer model; it represents a significant addition of TKE physics to the first two models. Equations for diurnal heating and cooling and three for energy transformation were added, and the W_e equation was reformulated. The resultant equations are:

$$Q_0 = -Q_a + Q_a \pi \left(\max\left(0, \cos\frac{2\pi t}{86400}\right)\right) \quad (7)$$

$$\frac{\partial \overline{u^2} h}{dt} = 2 m_3 u_*^3 + U^2 W_e + 2 m_2 (E - 3\overline{u^2})\sqrt{E} - \frac{2}{3}\left(m_1 E^{\frac{3}{2}} + m_5 f h E\right) \quad (8)$$

$$\frac{\partial \overline{v^2} h}{dt} = V^2 W_e + 2 m_2 (E - 3\overline{v^2})\sqrt{E} - \frac{2}{3}\left(m_1 E^{\frac{3}{2}} + m_5 f h E\right) \quad (9)$$

$$\frac{\partial \overline{w^2} h}{dt} = -\alpha g h \Delta T W_e - \frac{\alpha g h Q_0}{\rho C_p} + 2 m_2 (E - 3\overline{w^2})\sqrt{E} - \frac{2}{3}\left(m_1 E^{\frac{3}{2}} + m_5 f h E\right) \quad (10)$$

$$W_e = \sqrt{\overline{w^2}}\,\frac{E}{\alpha g h \Delta T + E} \quad (11)$$

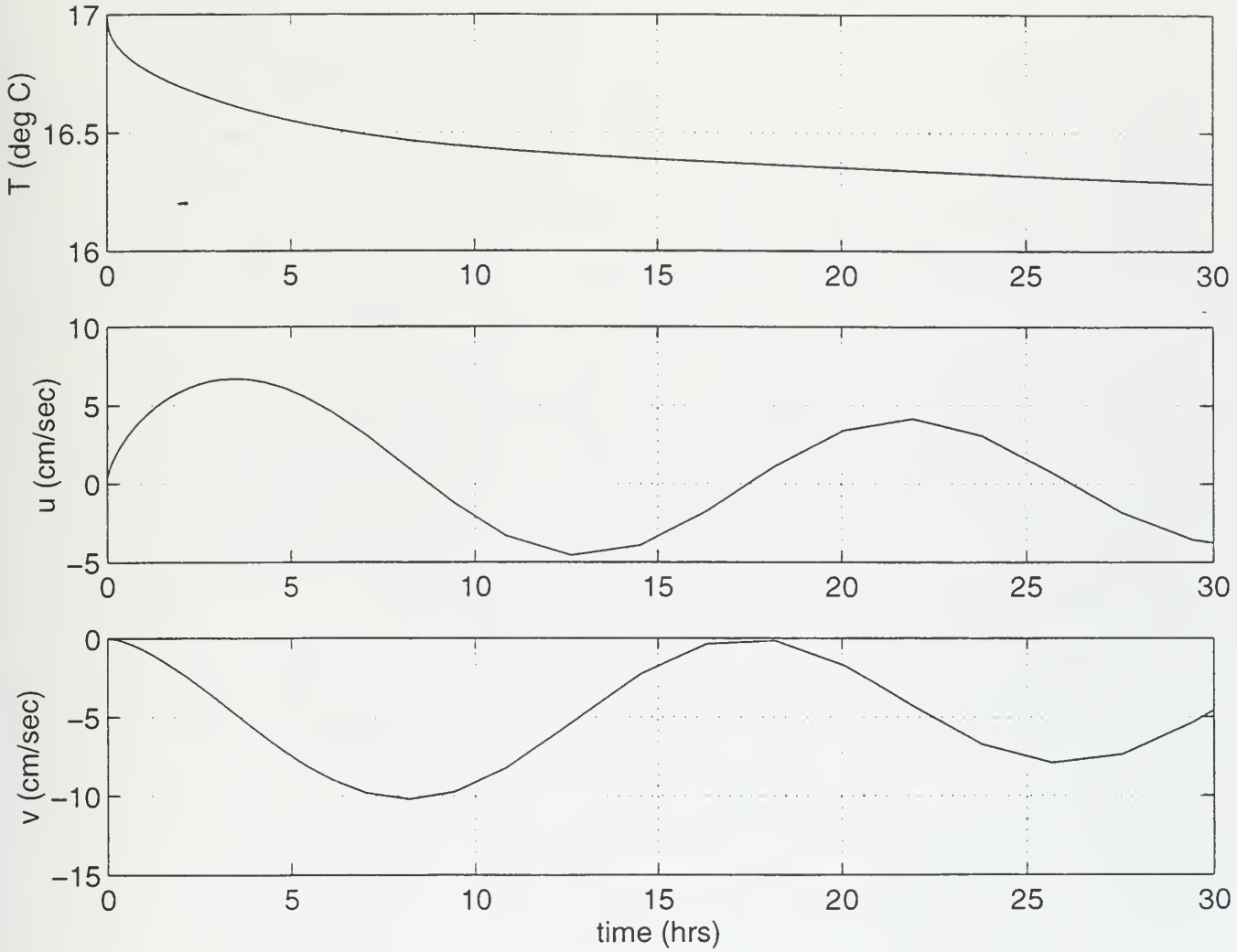

Figure 2.3 Solution for temperature and velocity.

$$\frac{\partial h}{dt} = W_e - W(z=-h) \qquad (12)$$

A $Q_o(t)$ equation (7) was designed to have a diurnal structure with a net zero heat flux. The energy transformation terms (m_2) redistribute energy among components, representing pressure-strain interactions. The variable E is the summation of the squares of the turbulent velocity fluctuations in the x, y, and z directions, $E=\overline{u^2}+\overline{v^2}+\overline{w^2}$. In equation (8), $m_3u_*^3$ is the near surface wind shear production term. The summation of the three $m_1E^{3/2}$ + m_5fhE terms found in equations (8),(9), and (10) is the viscous dissipation. The $m_3u_*^3$ term and the summed $m_1E^{3/2}$ + m_5fhE terms are approximated in the de Szoeke and Rhines equation by the $m_0u_*^3h$ term. The $m_2(E-3u^2)E^{1/2}$ terms are pressure redistribution of TKE among the components, in which the turbulence tends toward isotropy by pressure-strain interactions. The $\alpha gh\Delta TW_e$ term in equation (10) is the buoyant damping of TKE by entrainment and corresponds to de Szoeke and Rhines N^2h^4 term. The $\alpha ghQ_0/\rho C_p$ term in equation (10) is the buoyant damping of TKE by surface heating (Q_0), and has no corresponding term in equation (1), although it was included in equation (6) of the second model. Equation (11) is the entrainment rate as a function of the ambient TKE. Equation (12) is the rate of change of the mixed layer due to entrainment, W_e, and vertical mean advection by W(z=-h).

Initial runs of this model were conducted with a constant wind stress but no heating or cooling. These solutions were similiar to the results of models one and two, but the mixed layer depths were significantly shallower (Figure 2.4). This is as expected and is attributed to energy being expended for turbulence spin up and dissipation in the layer as well as entrainment. Two differences between the first and third models are significant: (i) calculation of dissipation and (ii) role of inertial oscillations.

Term D, in the de Szoeke and Rhines model, near-surface wind shear production of TKE minus viscous dissipation, is an over simplification. The viscous dissipation should not be represented as directly proportional to $u_*^3 h$. The dissipation resulting from the shear production due to entrainment is not represented at all. Figure 2.5 is analogous Figure 2.1, and it shows the spin up of model terms. The ratio of D3/A3 is near-surface wind shear production of TKE minus viscous dissipation over buoyant damping of TKE by entrainment. The ratio of B3/A3 is shear production of TKE by entrainment over buoyant damping of TKE by entrainment. The ratio C3/A3 is the turbulence spin-up term over buoyant damping of TKE by entrainment. The most obvious difference is in the ratio D3/A3. Total dissipation is much larger in the third model than with the approximation used in the first model because

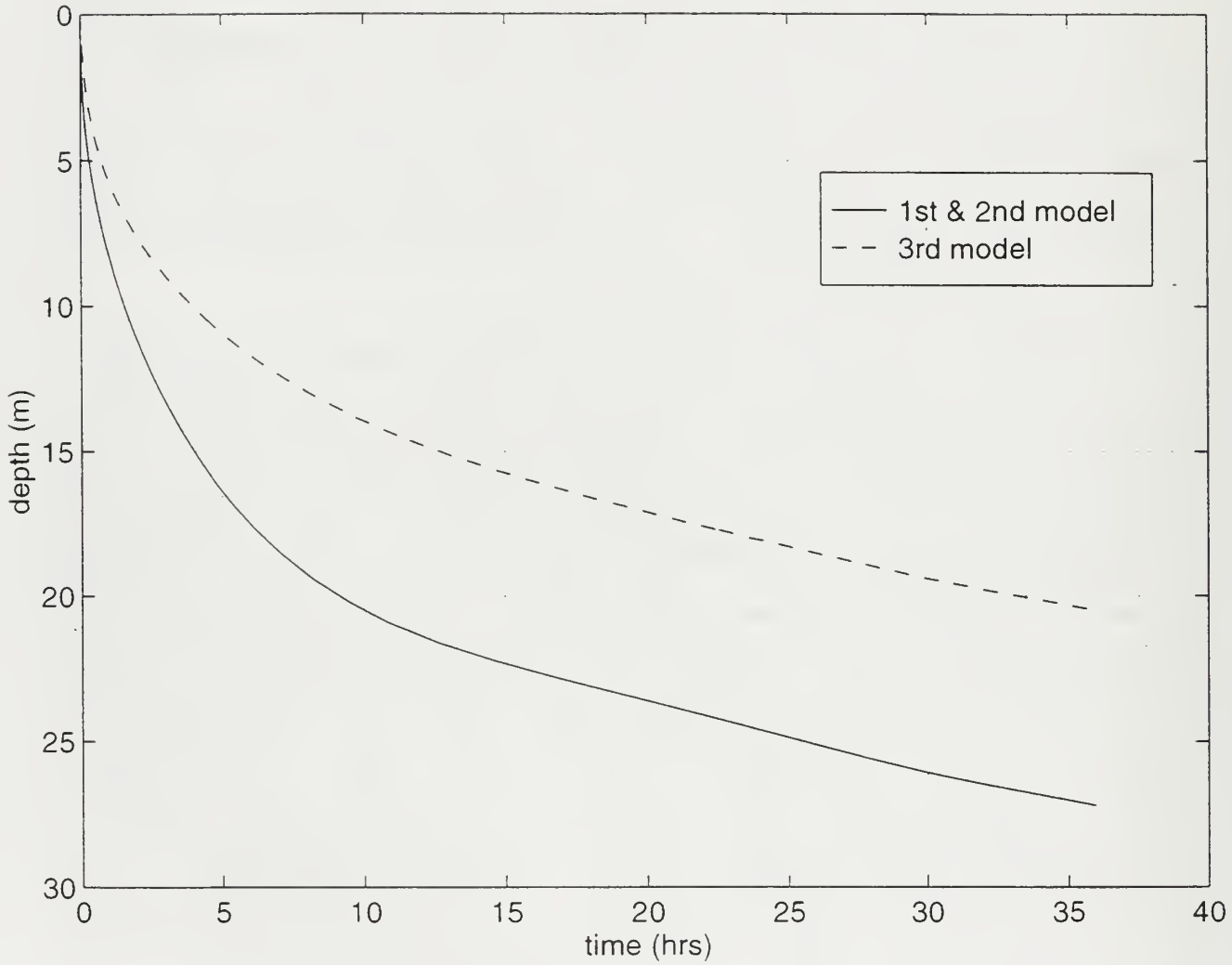

Figure 2.4 Comparison of mixed layer depths between model two and model three.

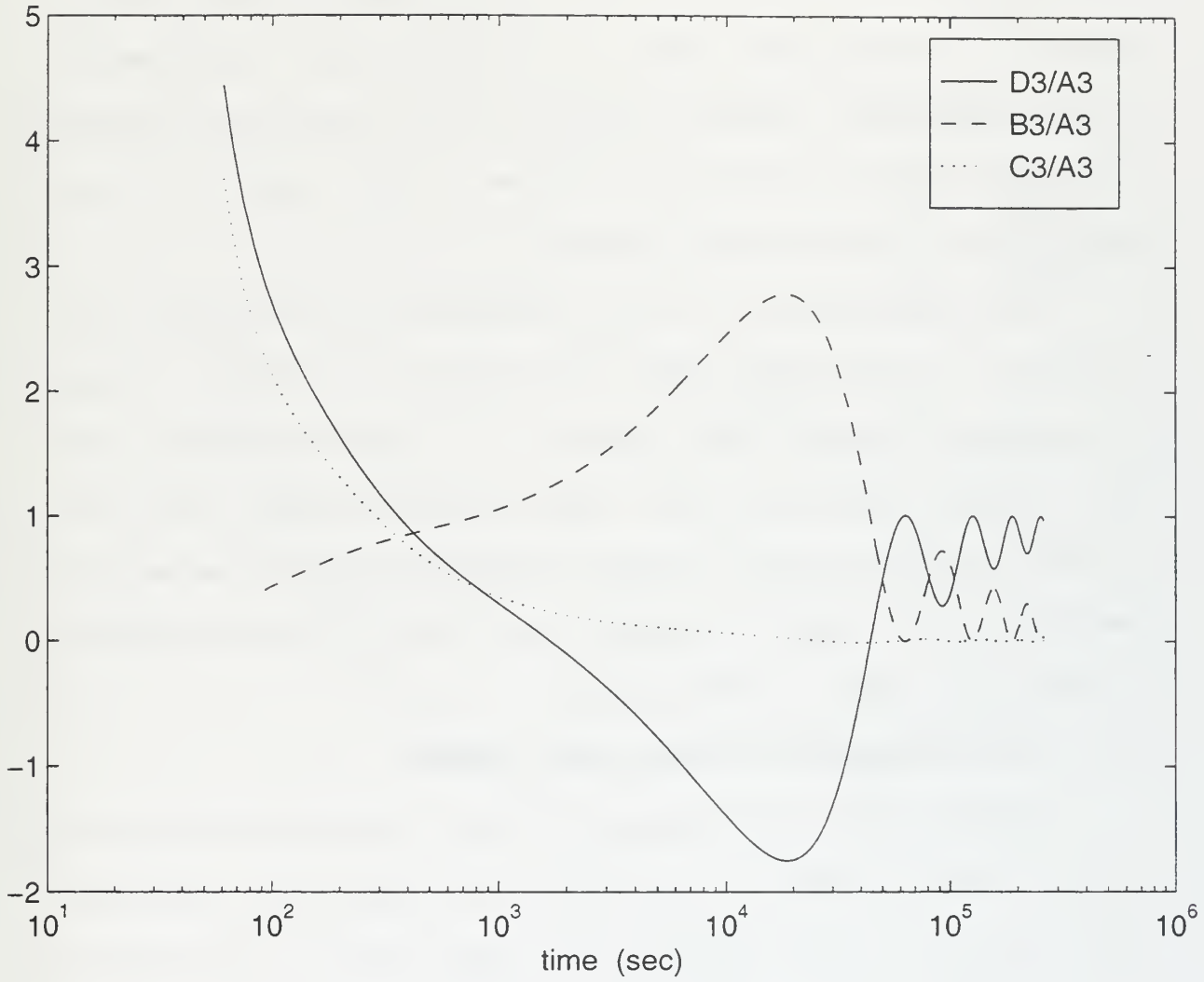

Figure 2.5 Model three solution. The ratios represent the same physical processes as Figures 2.1a and 2.1b.

the first model estimated viscous dissipation as proportional to the wind stress only. The third model calculates the dissipation for all three TKE components based on the explicitly calculated TKE in the mixed layer. Between 10^3 seconds and $4x10^4$ seconds, there is more viscous dissipation than wind shear production, because of the addition of the dissipation due to shear production.

The significance of term B decreases as the mixed layer deepens. In the first model, the effect of inertial forcing is negligible after $6x10^4$ seconds. In the third model, term B3 remains significant four times longer than for model one. If the dissipation due to shear entrainment is neglected, the amplitude of term B3 decreases, and term A3 and D3 dominate (Figure 2.6) after $1x10^5$ seconds.

D. MODEL RESOLUTION IN THE TIME DOMAIN

Models one through three all use a Runge-Kutta solution with a variable time step to solve the mixed layer equations. The numerical scheme maximizes the time step to solve the set of equations without exceeding specified error tolerances. In mixed layer physics, $\partial h/dt$ is not a continuous function when mixed layer shallowing occurs. For this reason, the Runge-Kutta solution can only be used during periods of mixed layer deepening. To study realistic cases, a model that can shallow as well as deepen was required.

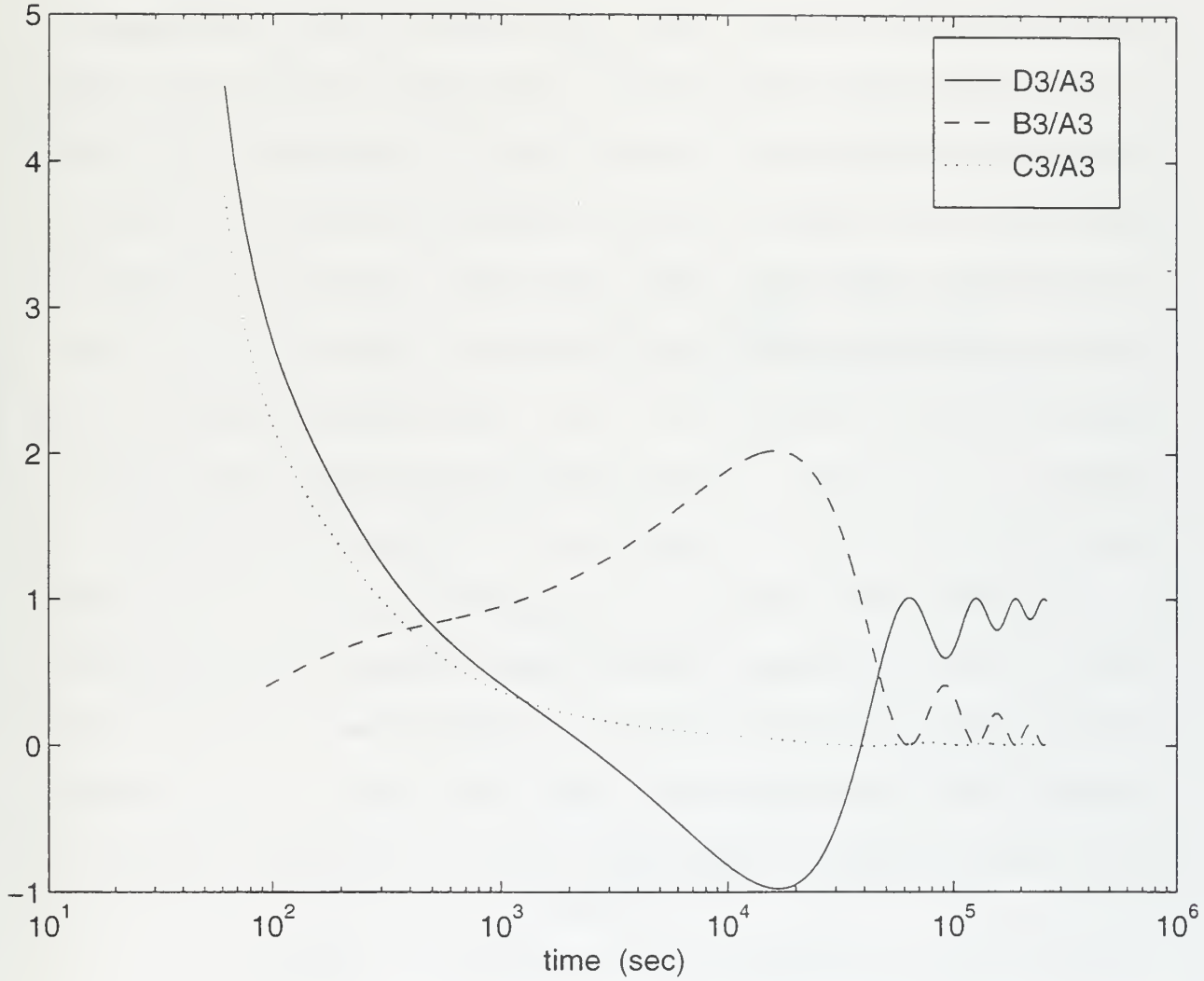

Figure 2.6 Model three solution with viscous dissipation Coriolis parameter m_5=0.

The NPS mixed layer model was chosen. The NPS model is a FORTRAN-based gridded numerical model with a fixed time step of one hour. Using a fixed time step to simultaneously solve differential equations introduces errors. To determine the adequacy of the one-hour time step, the NPS model was compared to the third model using mixed layer depth (Figure 2.7) and temperature (Figure 2.8) as the basis of comparison. The NPS model does not have a term for shear production of TKE by entrainment (term B3) but vertical mixing by dynamic instability occurs when the Richardson number (Ri) is less than the critical value, Ri < 0.25, following the procedure of Adamec et al. (1981). These physical processes can then be selectively included or neglected for comparison purposes.

The NPS model deepens too quickly during the first time step. This is because the NPS model assumes fully spun-up steady state turbulence. This is accomplished by solving the steady state equations (13), (14), and (15), or by setting the left hand side of equations (8), (9), and (10) to zero.

$$0 = V^2 W_e + 2m_2 (E - 3\overline{v^2})\sqrt{E} - \frac{2}{3}(m_1 E^{\frac{3}{2}} + m_5 f h E) \qquad (13)$$

$$0 = -\alpha g h \Delta T W_e - \frac{\alpha g h Q_0}{\rho C_p} + 2m_2 (E - 3\overline{w^2})\sqrt{E} - \frac{2}{3}(m_1 E^{\frac{3}{2}} + m_5 f h E) \qquad (14)$$

$$0 = 2m_3 u_*^3 + U^2 W_e + 2m_2 (E - 3\overline{u^2})\sqrt{E} - \frac{2}{3}(m_1 E^{\frac{3}{2}} + m_5 f h E) \qquad (15)$$

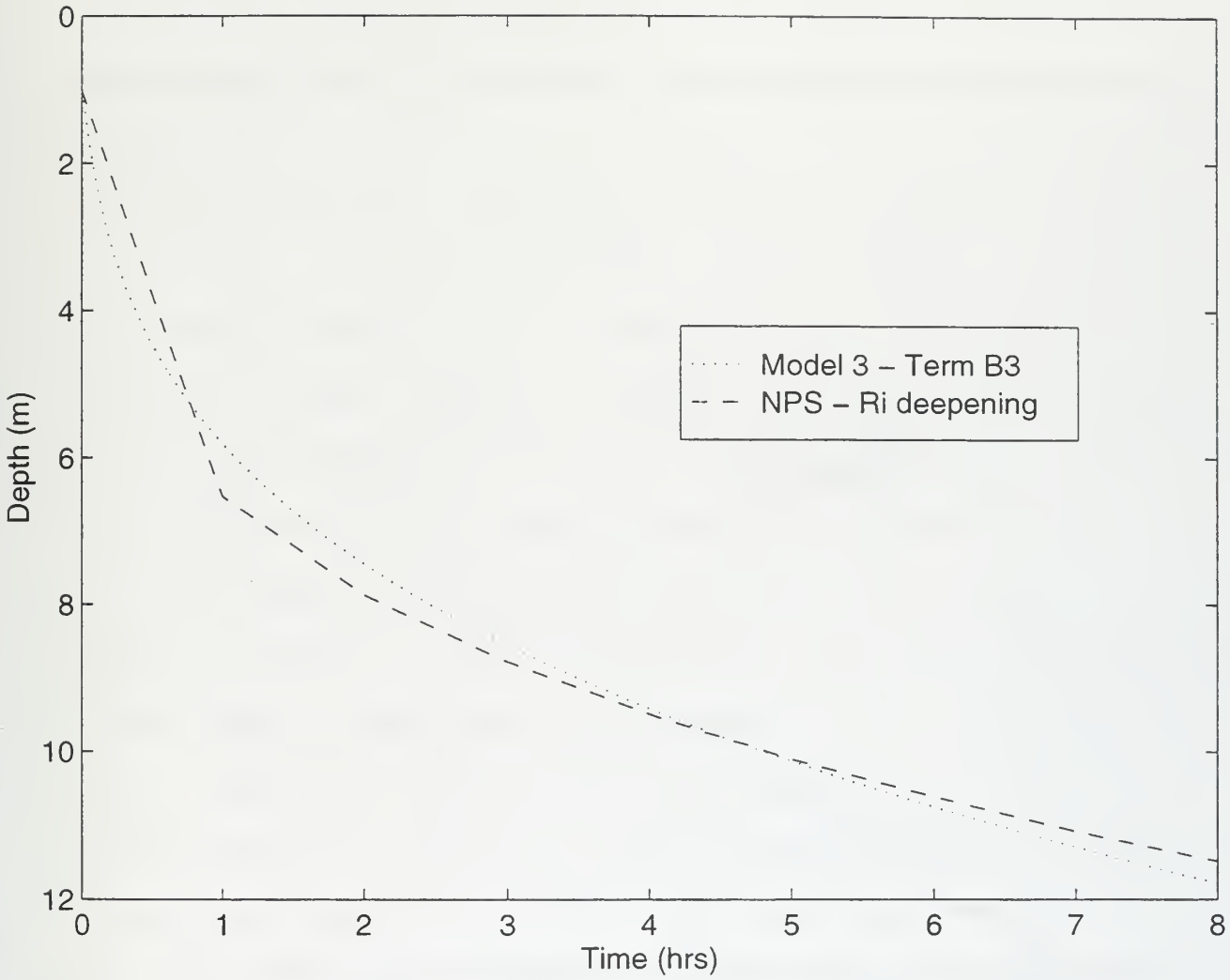

Figure 2.7 Mixed layer depth comparison between the NPS mixed layer model with Richardson Number deepening turned off and model number three with Term B3 turned off.

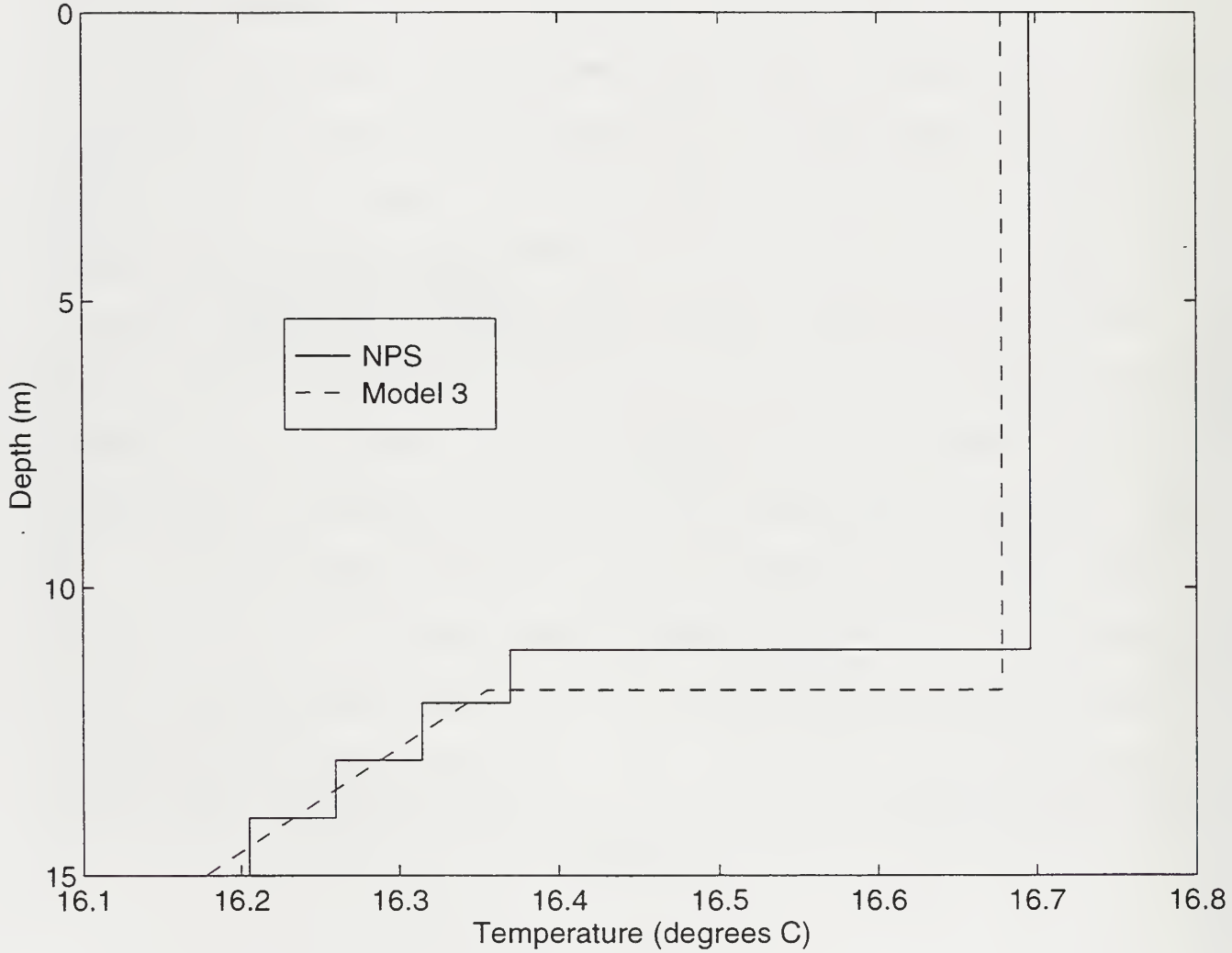

Figure 2.8 Mixed layer temperature comparison between the NPS mixed layer model and model number three, at time = 8 hours.

This assumption allows instantaneous deepening to occur without having to spin up the turbulence. Depending on the rate of fluctuation in the forcing, this may not be a valid assumption. Figure 2.9 depicts a portion of the C3/A3 ratio from Figure 2.5. Examination of the results depicted in Figure 2.9 reveals that the unsteady term does not approach zero at 10^4 seconds as proposed by de Szoeke and Rhines but at 10^5 seconds. At 0.36×10^4 seconds, this assumption results in a maximum 14 percent error in TKE generation for any change in forcing. If the forcing is constant or slowly changing this error is negligible. Figure 2.9 indicates that the unsteady term persists and oscillates in excess of 3 days.

The temperature profiles differ for two reasons. The first is related to mixed layer depth. The NPS mixed layer model depth is shallower and therefore warmer. Conversely, model three has a deeper mixed layer depth and is cooler. The second reason is related to model thermal structure. Model three has a continuous function for temperature versus depth. The NPS model is a gridded model and assumes a step like function for temperature. The difference in thermal structure between the models is evident in Figure 2.8 in the region below the mixed layer.

To further test the adequacy of the one hour time step, the NPS model was run with a 15 minute time step. The results

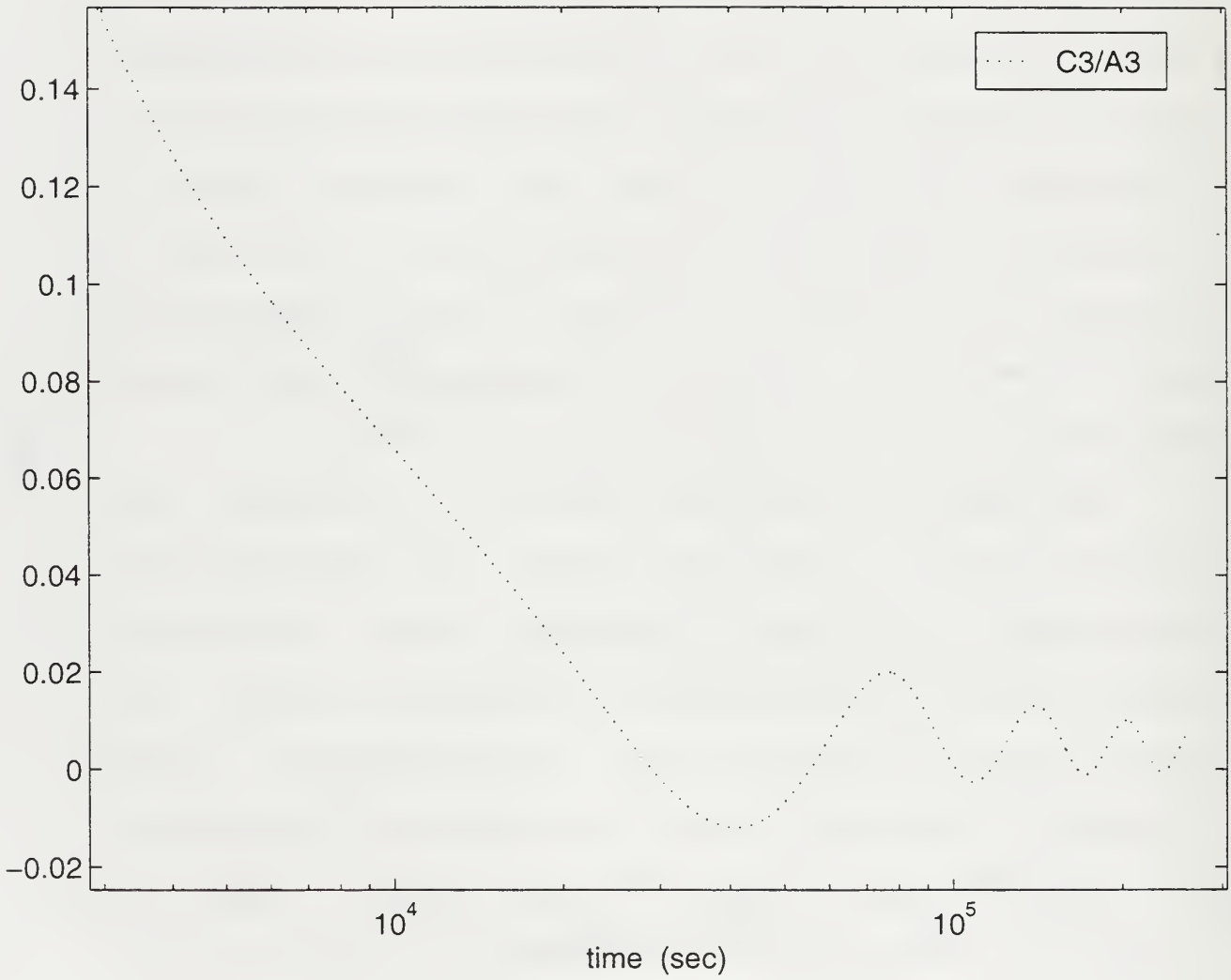

Figure 2.9 Ratio of Model three turbulence spin-up over buoyant damping of TKE by entrainment (C3/A3).

are depicted in Figure 2.10. After the second time step of the one hour model, the mixed layer depths of the two NPS models are parallel in time with an offset of approximately 0.5 m. The one-hour time step of the NPS mixed layer model is sufficient for the proposed study. This conclusion was reached because the error induced by the relatively large time step is small and explainable. After initial spin up, the 15 minute time step does not result in significant resolution improvement. Additionally, the subsequent forcing data to be used has a sampling period of three hours. Interpolating to time steps less than an hour was therefore judged to be inappropriate.

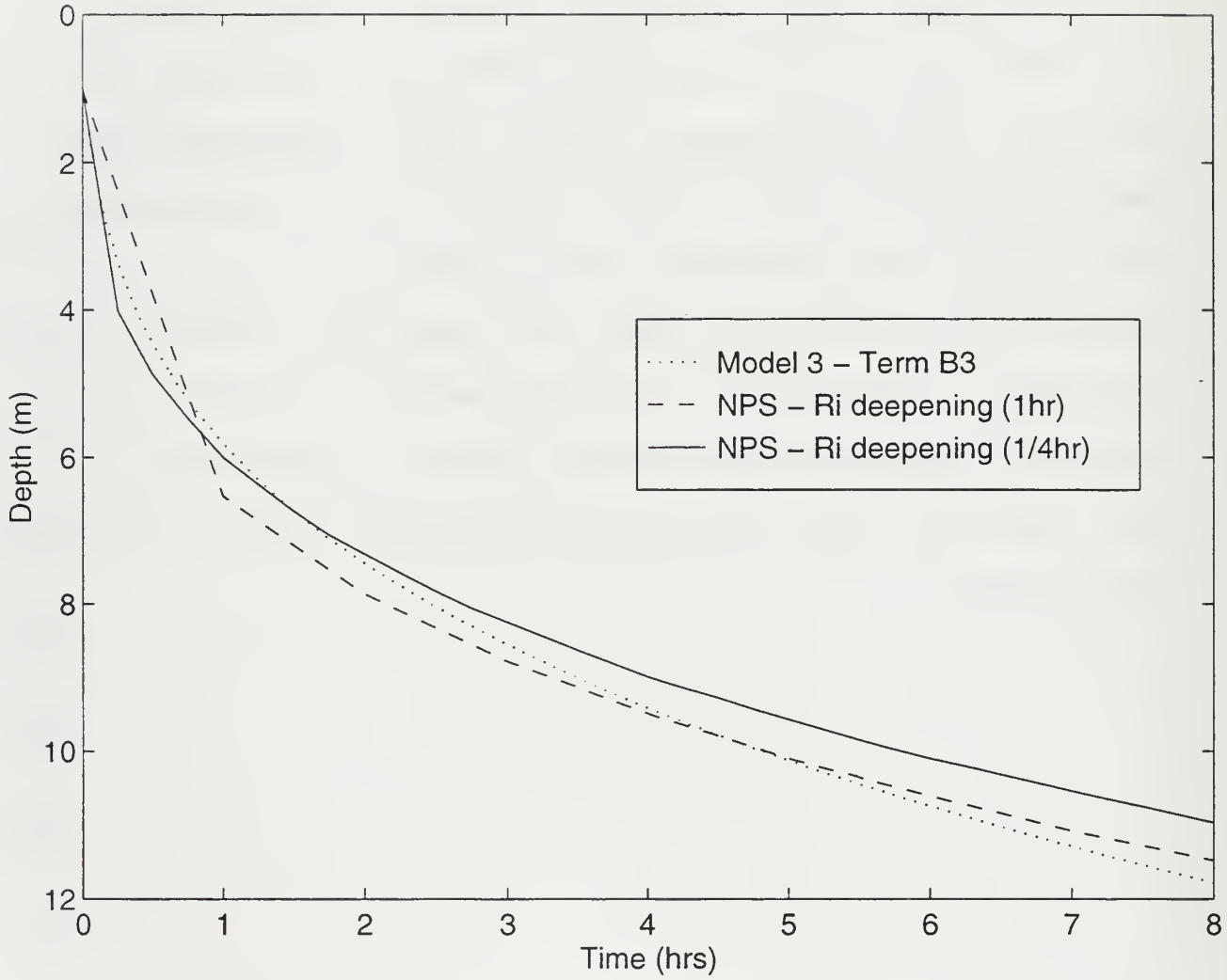

Figure 2.10 Mixed layer depth comparison using the one-hour time step and the 15 minute time step NPS mixed layer model, and model number three.

III. REALISTIC SOLUTIONS

A. IMPORTANCE OF VERTICAL RESOLUTION

In any geophysical process model, the resolution required is dependent on the scale of the physical phenomena to be represented. The annual fluctuation in the mixed layer depth at station Papa is on the order of 150 m. The daily fluctuations vary between order 10 m and order 100 m, depending on time of year and the synoptic forcing. Unlike other mixed layer models, the NPS mixed layer model used here employs a floating grid point assigned to the mixed layer depth to increase the model's resolution. This feature becomes more significant as grid size increases.

The choice of vertical grid spacing (Δz) is governed by several factors. The two factors considered in this thesis are model computational speed and resolution. These two factors are not independent of each other. Smaller grid spacing requires increased computer time, but resolves more features; larger grid spacing is faster, but has reduced resolution. Model requirements will determine which one of these two factors is more important. In the past, embedding a mixed layer within an ocean general circulation model or coupling a well-resolved upper ocean model to a global atmospheric model has been prohibitive because of the number

of grid levels required to represent the ocean. The following sections address the question of required vertical grid spacing and the accuracy of larger grid sizes.

B. MODEL FORCING

The atmospheric forcing utilized was calculated from observations by a Canadian weather ship in the vicinity of 50° North latitude 145° West longitude, nominally referred to as station Papa. Three hourly weather observations were taken, consisting of wind speed and direction, air and sea surface temperature, dew point, and fractional cloud cover. The three-hourly observations were interpolated to hourly values. Aerodynamic bulk formulas derived by Large and Pond (1982) and modified by Oberhuber (1993) were used to compute the momentum, sensible, and latent heat fluxes, correcting for atmospheric stability. Mechanical bathythermographs(MBT) were also taken at irregular intervals at station Papa, varying from less than an hour to several days. The MBT data was manually digitized at 5 m intervals. The MBT data are used in this study to initialize the mixed layer model and then for subsequent verification. Model runs were conducted for various periods between 1961 and 1969. In addition to being one of the longest running continuous oceanic time series, the data set is ideally suited to testing a one dimensional model

because the horizontal currents are weak and advection due to upwelling is generally believed insignificant (Tabata, 1965).

C. EFFECT OF VERTICAL GRID SIZE

The 1 m grid NPS mixed layer model has a minimum mixed layer depth of 1 m, or one Δz. Changing the grid spacing raised the issue of what the minimum mixed layer depth or ceiling should be. When Δz was increased to 10 m and 20 m, a 1/4 Δz minimum mixed layer depth was found to be optimal. The 1/4 Δz ceiling resulted in a 30% decrease in mean error in temperature over the one-Δz ceiling. In the presence of strong heating and no wind stress, ceilings smaller than 1/4 Δz resulted in the mixed layer temperature becoming unrealistically hot. The same unrealistic temperatures were also obtained in the 1 m grid case by raising the ceiling above one Δz.

D. VERIFICATION WITH OBSERVATIONS

1. Model Predicted SST vs Bucket Temperature

Sea surface temperature is the only state variable for which model output and station Papa observations can be continuously compared. To accomplish this task, the model mixed layer temperatures were compared to the interpolated bucket temperatures. The mean difference and standard deviation were used for comparison.

$$\text{The mean difference} \equiv \frac{\sum_n (SST_{calc} - SST_{bucket})}{n}$$

The mean difference calculation was used to evaluate the effect of varying the minimum allowable mixed layer depth as described in section III C. The results presented in Appendix A provide the justification for selecting 1/4 Δz as the minimum ceiling for Δz's of 10 m and 20 m. The eight annual-period model runs commenced in mid-March, near the time of maximum mixed layer depth, and ran for 365 days. The results of the mean differences were unexpected and raised questions about optimal spatial resolution. In every case but one, the error for model runs with 1 m grid spacing was greater than for both the 10 m and 20 m Δz cases. This implies that the coarser grid is more accurate. The standard deviation showed the same trend. The model runs depicted in Figure 3.1 are characteristic of the other years. Spectra were calculated for 1 m, 10 m and 20 m grid resolution(Figures 3.2, 3.3, & 3.4, respectively). The annual cycle was not resolved due to the spectral computational length of the time series; however, the diurnal cycle is evident. The diurnal cycle was best resolved by the 10 m grid, then by the 20 m grid, and lastly by the 1 m grid.

In an attempt to understand why better model performance is achieved with coarse resolution, model tuning sensitivity

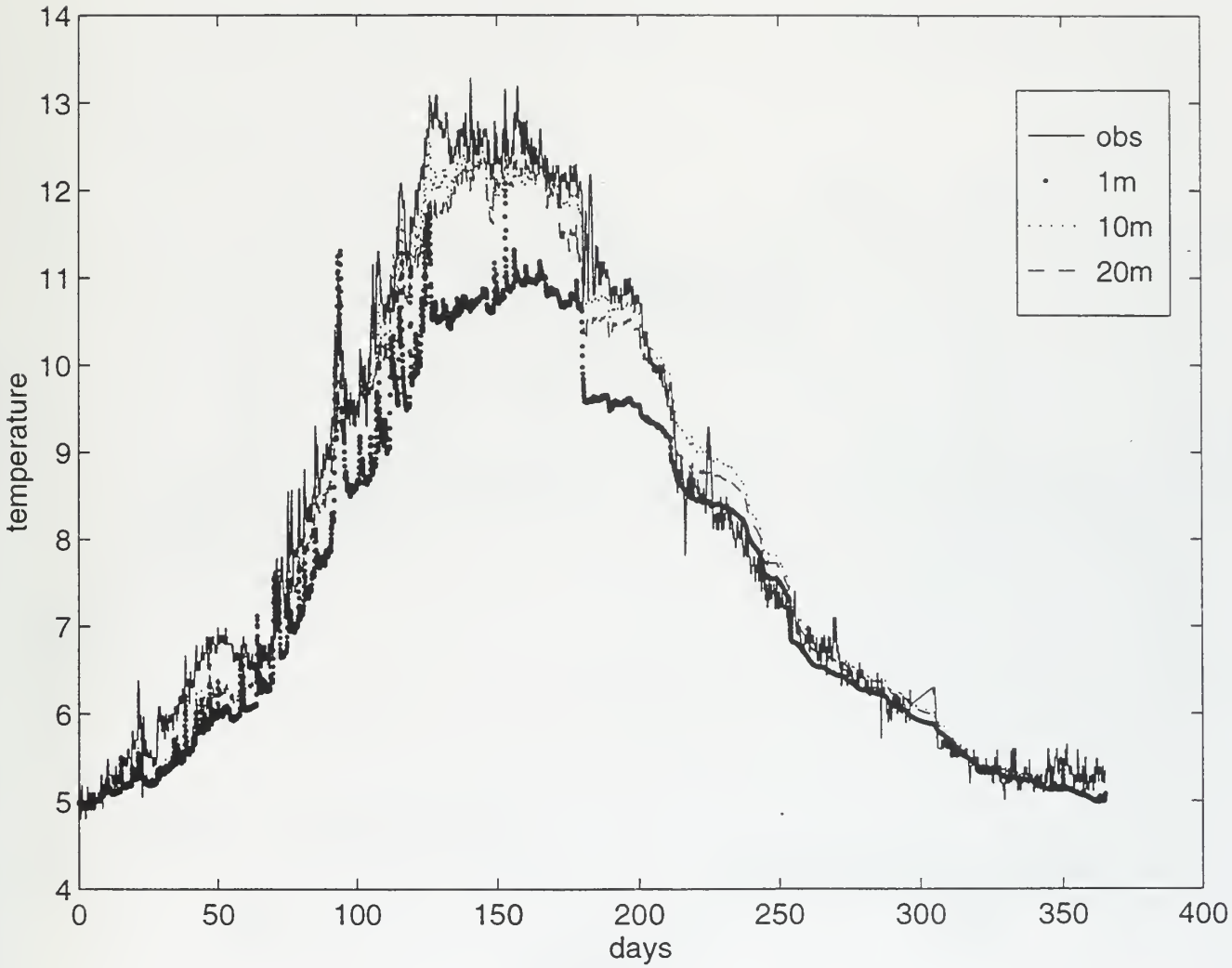

Figure 3.1 Observed bucket temperatures and model output for 1966.

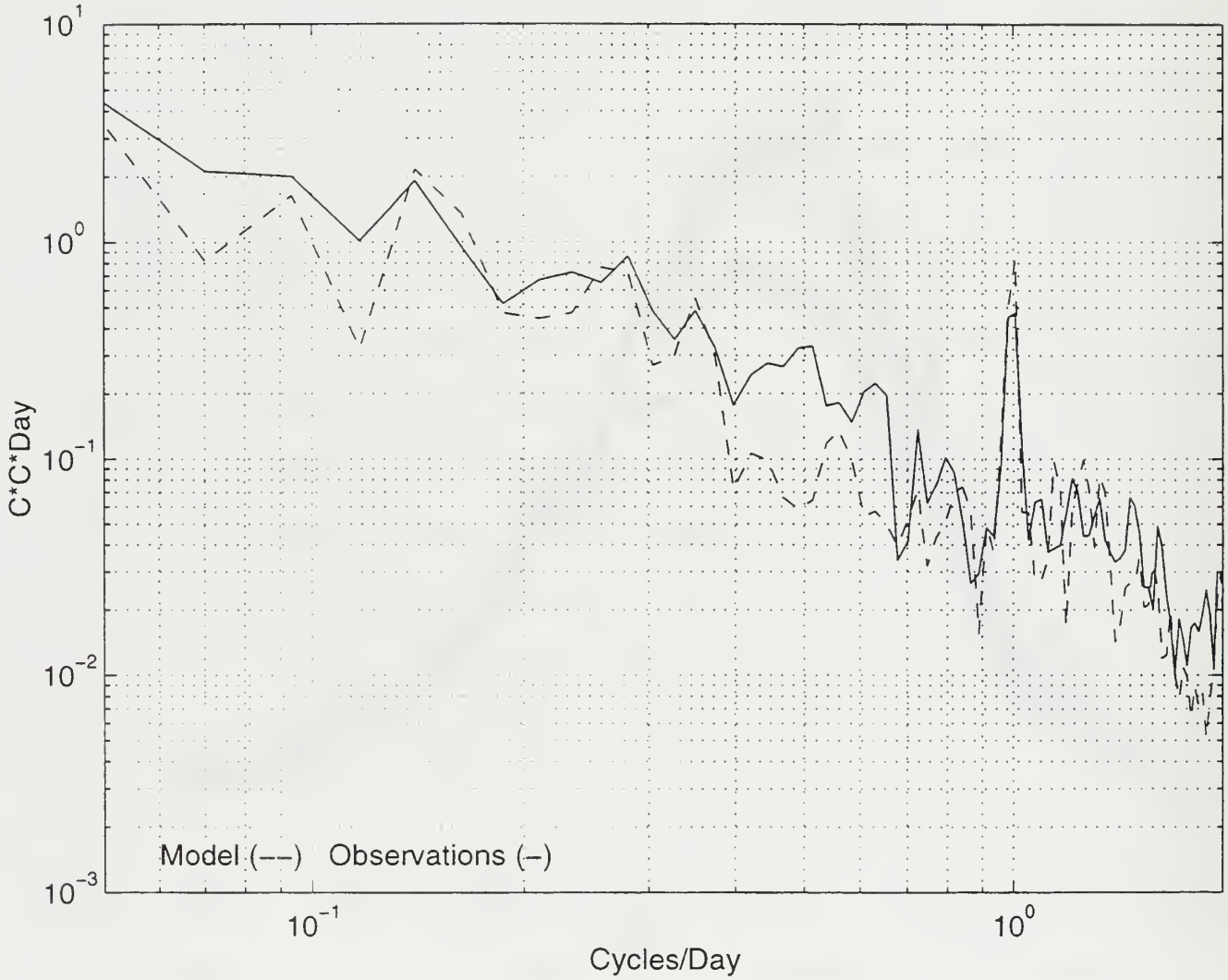

Figure 3.2 Spectra for 1 m grid spacing for 1966, using tunning coefficients P3 = 4.6 and AM3 = 4.5.

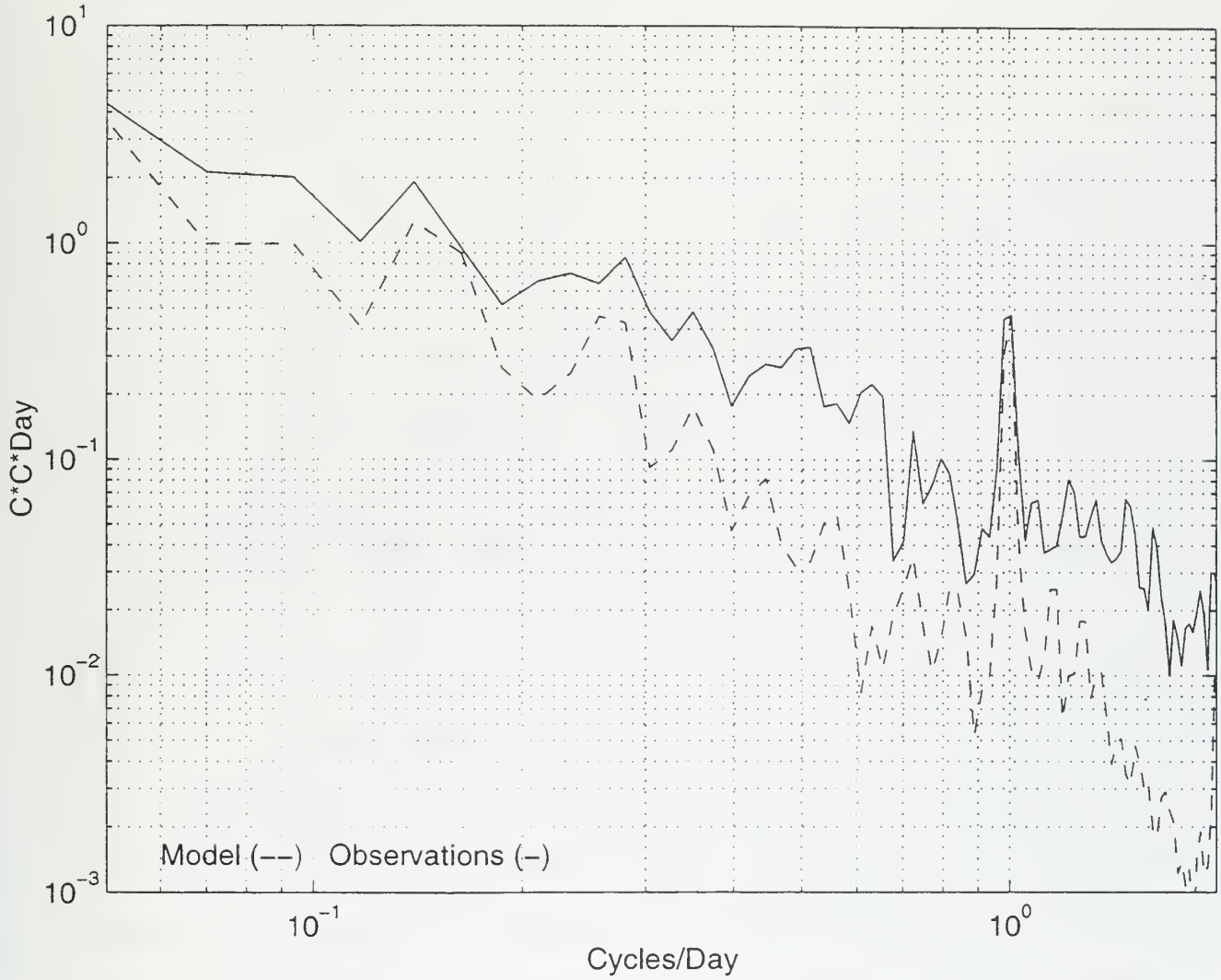

Figure 3.3 Spectra for 10 m grid spacing for 1966, using tunning coefficients P3 = 4.6 and AM3 = 4.5.

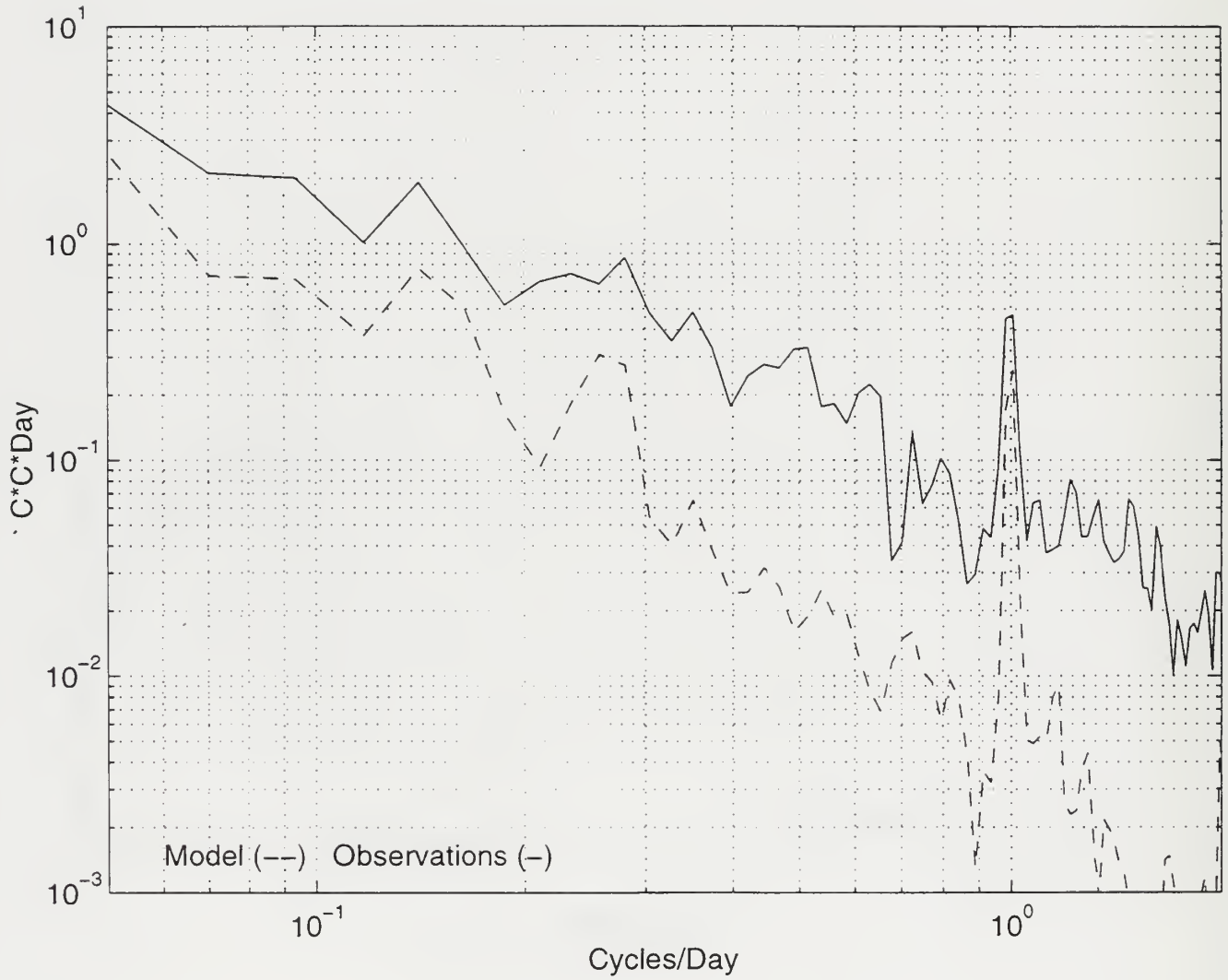

Figure 3.4 Spectra for 20 m grid spacing for 1966, using tunning coefficients P3 = 4.6 and AM3 = 4.5.

tests were conducted. Tuning coefficients P3 and AM3 in equations (13), (14), and (15) were varied, and the model rerun for each year. Tuning coefficient P3 equals m_5/m_1, and regulates the effect of the Coriolis in the dissipation term; larger P3 results in stronger dissipation. Tuning coefficient AM3 equals m_3 and regulates the efficiency of shear production. Larger AM3 results in increased shear production.

Year-long model runs for eight years were made for each P3 and AM3 pair. The values ranged for 3 to 8 for P3 and 1 to 9 for AM3. The standard deviation for each run was calculated and the results averaged. Figure 3.5 depicts the average error for the 1 m grid spacing cases; Figures 3.6 and 3.7 depict the average error for the 10 m and 20 m grid spacing respectively. A well-defined region of minimum error is evident for the Δz equal to 10 m and 20 m cases. This same region is not as clearly defined in the Δz equal to 1 m case.

Optimal tuning parameters were chosen which represent the (P3, AM3) region of minimum error. The model was rerun for five different time frames and for seven different tuning coefficient pairs. The first was a repeat of the annual cycle. The next four were 10 day runs, one per season. This was done not only to elucidate differences in model accuracy among the seasons, but also to determine if the 1 m Δz model improved over the larger grid models for diurnal and synoptic

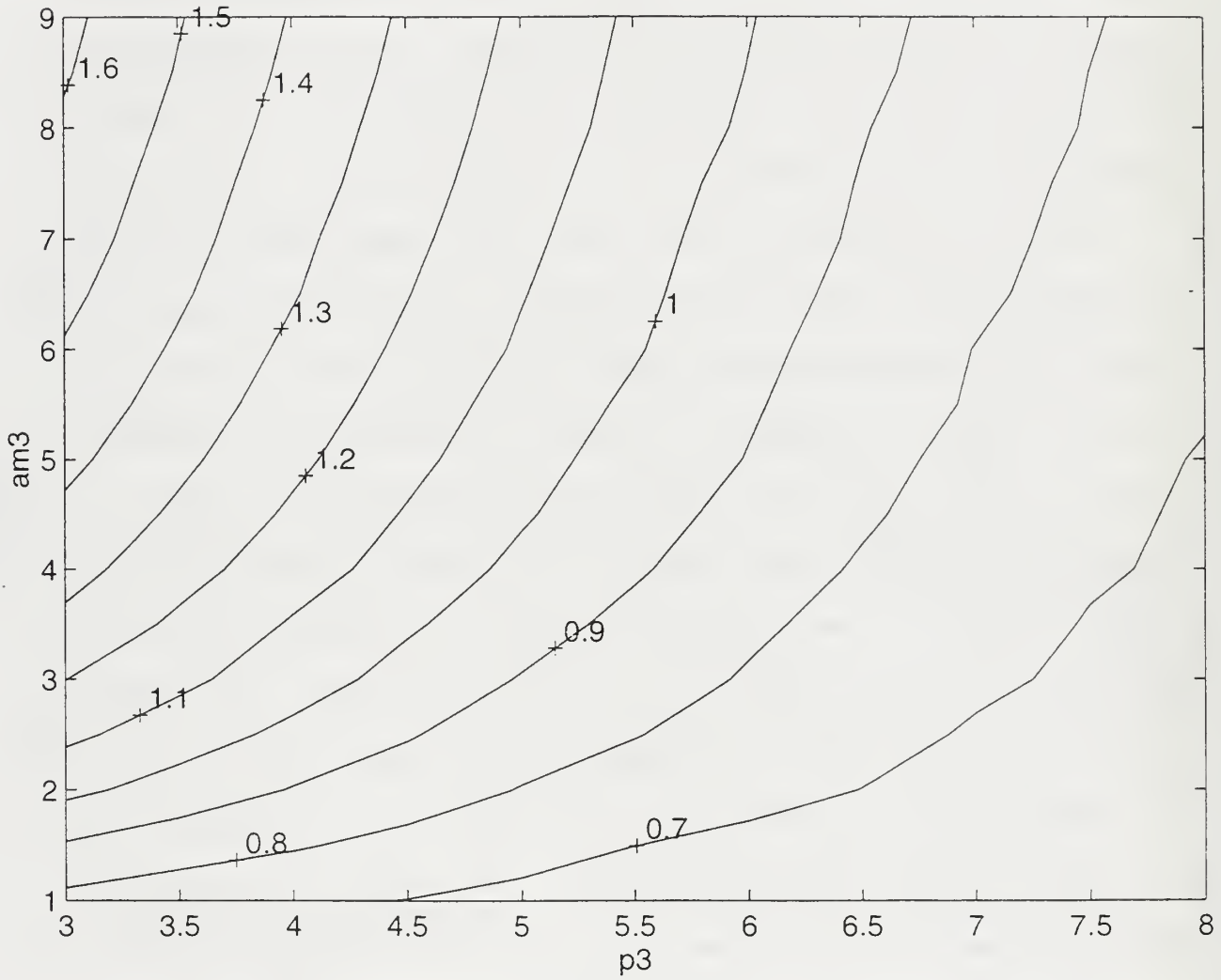

Figure 3.5 Average standard deviation error (° C) for 1 m grid spacing.

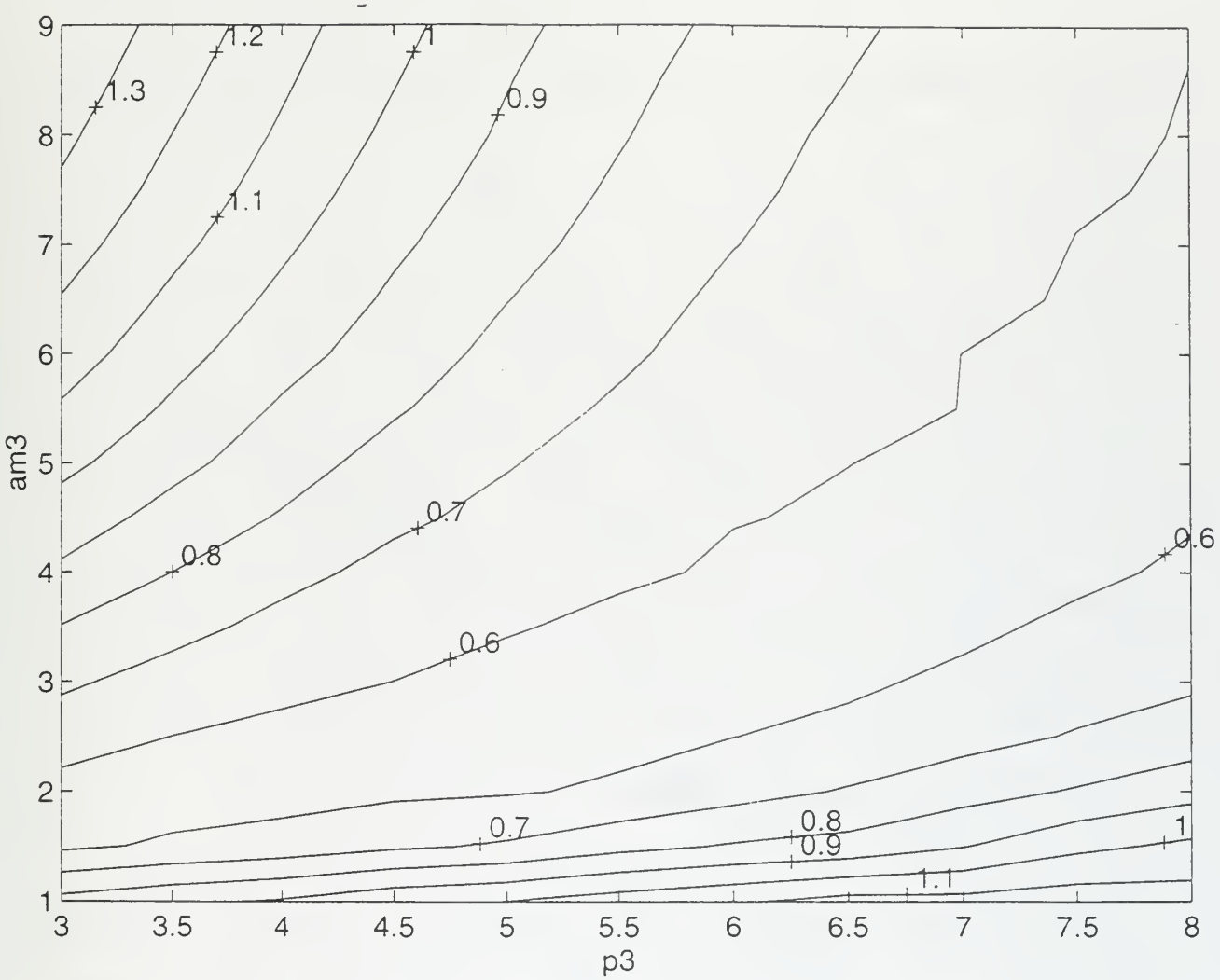

Figure 3.6 Average standard deviation error (° C) for 10 m grid spacing with a ceiling of 2.5 m.

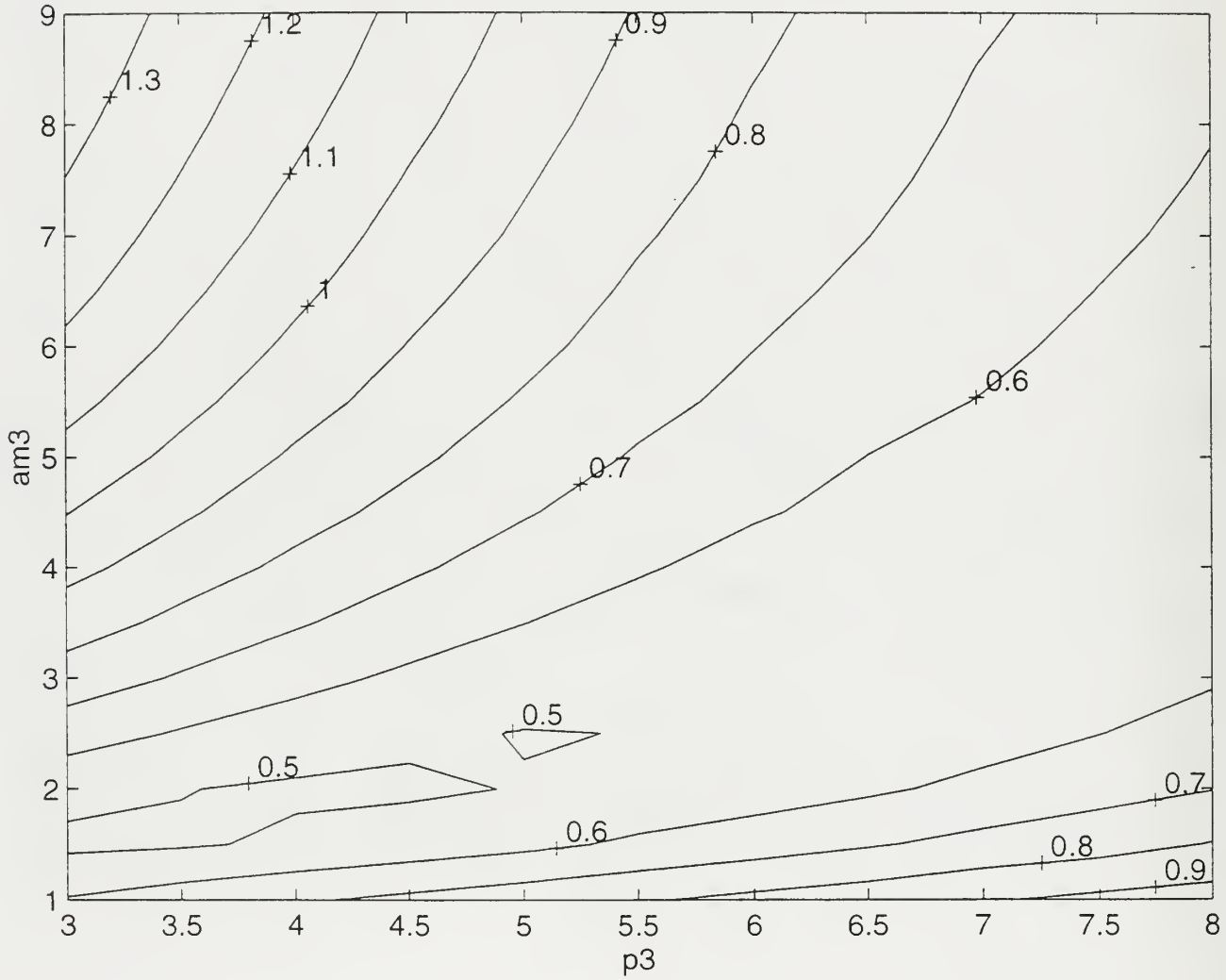

Figure 3.7 Average standard deviation error (° C) for 20 m grid spacing with a ceiling of 5 m.

scales. The standard deviations were calculated and tabulated. Appendix B is the complete listing of results by tuning factor pairs.

The results of the in-depth tuning study are both clarifying and conclusive. The vertical grid spacing accuracy is dependent on time of year and length of model run (see table 1). During the spring and summer when the forcing is dominated by the diurnal cycle, the larger Δz's are more accurate. During the synoptically forced deepening period of the fall, the 1 m grid spacing more accurately represents the bucket temperatures. In the 48 cases where the grid size is a factor when using 10 m vice 1 m Δz, an increase in standard deviation error of 0.06° C resulted, and an increase of 0.05° C resulted in the 35 cases when 20 m Δz were used. The winter accuracy is generally independent of grid spacing.

2. Bucket vs Mechanical Bathythermograph SST

The NPS mixed layer model uses BT's to initialize the model. After initialization, surface meteorological observations are used to drive the model. The surface observations were taken at 3 hourly intervals, but the MBTs were deployed at irregular intervals. For initial conditions, the model uses the BT with the closest Julian date to the start date of the run. In general the relative vertical structure of the surface layer will be correct, but a random

bias in the absolute temperature will be induced. Additionally, a phase shift is also likely, as the model starts at 00 GMT and the BT may or may not be at 00 GMT. Figure 3.8 demonstrates the bias between bucket and BT temperatures and the irregular sampling interval of the BTs.

Δz / Time	1 m	10 m	20 m	1 m & 10 m	1 m & 20 m	10 m & 20 m	1 m 10 m 20 m
Year	10	33	11	0	0	2	0
Spring	0	12	6	0	1	15	22
Summer	2	7	31	5	2	7	2
Fall	37	0	7	1	4	0	7
Winter	9	1	0	0	0	2	44

Table 1. Values represent the number of relative minima in standard deviation of the error. The last four columns account for model runs were the standard deviations of the error are equal.

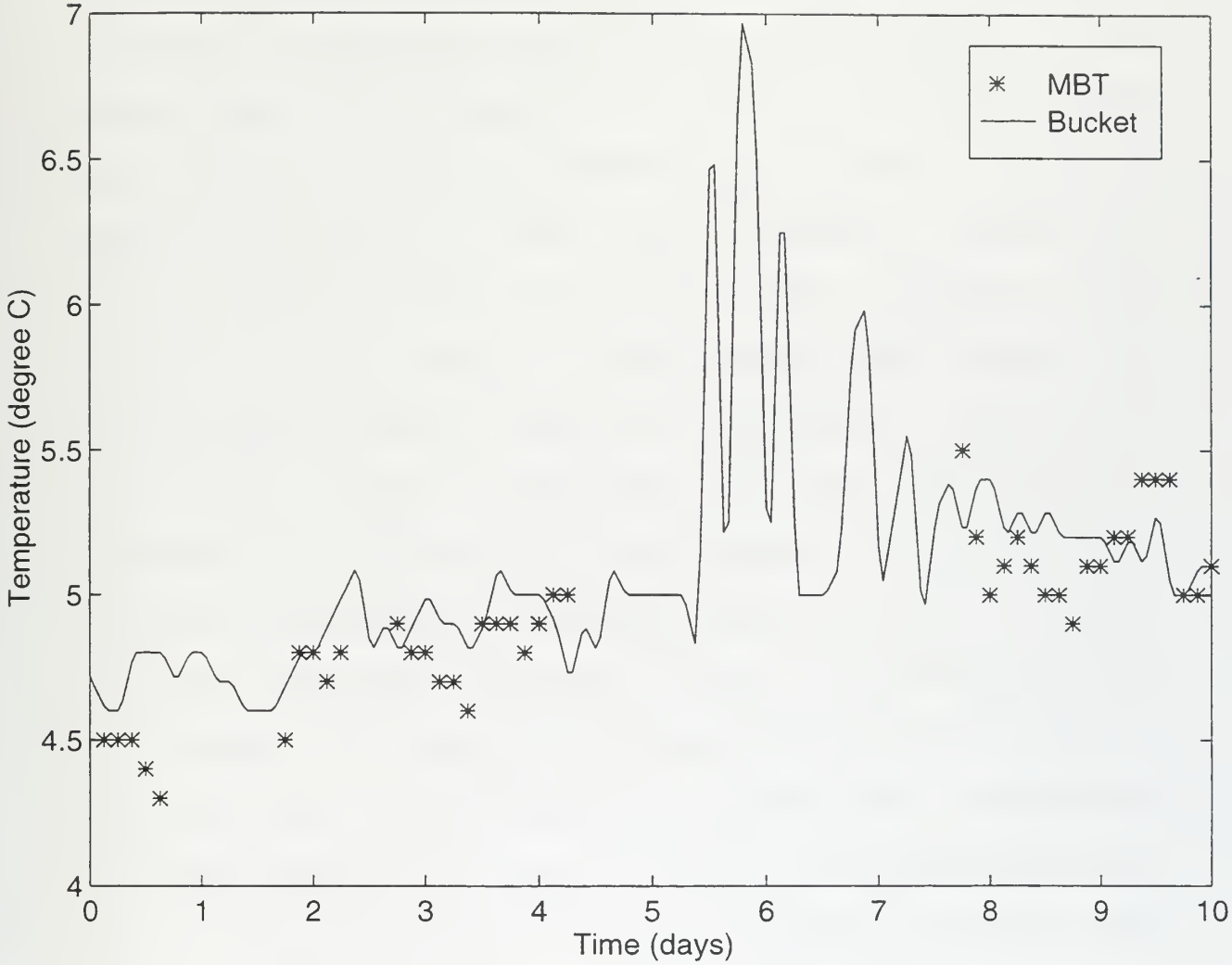

Figure 3.8 Example of bucket temperatures vs mechanical bathythermograph SST at station Papa.

IV. SUMMARY AND RECOMMENDATIONS

This study has evaluated the response of the ocean mixed layer to transient forcing and the time and space resolution required to accurately model upper ocean variability. This study began with replication of de Szoeke and Rhines (1976) work, using a Runge-Kutta MATLAB solution method. Additional physics were added to their model including: surface heat flux, improved viscous dissipation, and anisotropy in the three-dimensional turbulent kinetic energy (TKE) budget. The surface heat flux was added for completeness but was not extensively tested in evaluating the most rapid transient responses with a less than diurnal period. The refinement of viscous dissipation and TKE budget resulted in modification of de Szoeke and Rhines' findings. First, the unsteady TKE term is important for a minimum of 10^5 seconds rather than only 10^4 seconds. Next, viscous dissipation should not be approximated as being proportional simply to $u_*^3 h$. This parameterization fails to take into account buoyancy flux due to surface heat flux and entrainment. The time scale of the turbulence also plays a role in dissipation, and is not previously included. Finally, shear production due to entrainment remains significant for a minimum of one pendulum-day instead of the one-half pendulum-day of the de Szoeke and Rhines' study.

Expanding the investigation to model predictions longer than a day, the NPS FORTRAN mixed layer model was employed. The required temporal resolution of mixed layer models is dependent on the phenomena to be studied. This study focused on the diurnal, synoptic, and annual cycles, for which the one-hour time step of the NPS FORTRAN model is more than adequate to resolve. The one-hour time step is well matched with the larger vertical grid spacings. Further research is required to determine whether a one-hour time step is too coarse when used with 1 m grid spacing. If a time step shorter than one hour is to be used, the unsteady term may need to be added to the NPS FORTRAN model.

Finally, the question of spatial resolution was addressed. The initial hypothesis for this research was that smaller grid spacing would yield better results than larger grid spacing. The results reported in Appendix A and Table 1 were therefore unexpected. With the exception of the winter time frame, the 10 m and 20 m grid spacing generally equaled or out-performed the 1 m grid spacing. Use of the 20 m grid spacing during the winter resulted in an rms error of 0.05° C, which is smaller than the 0.1° C precision of the bucket temperatures. Overall, the NPS FORTRAN model skill was comparable for 1 m, 10 m, and even 20 m vertical grid spacing. Therefore, the conclusion of this thesis is that use of 10 m

and 20 m vertical grid spacing in global ocean models and coupled air-ocean models to represent the mixed layer is accurate and justified.

APPENDIX A. ANNUAL MEAN OF PREDICTED TEMPERATURE ERROR (DEGREES C) FOR VARIOUS MINIMUM ALLOWABLE MIXED LAYER DEPTH

Year	Δz	1 Δz	0.5 Δz	0.25 Δz	1.01 m
1961	1	-1.5698	-1.5537	-1.5257	-1.5644
	10	-1.0555	-1.0425	-1.0272	-0.9973
	20	-1.1308	-1.0693	-1.0514	-0.9948
1962	1	-0.4187	-0.3665	-0.3338	-0.3959
	10	0.1393	0.1937	0.2296	0.2859
	20	-0.0428	0.0795	0.1181	0.2257
1963	1	-0.2282	-0.2014	-0.1808	-0.2274
	10	0.3013	0.3154	0.3331	0.3608
	20	0.1765	0.2451	0.2680	0.3266
1964	1	-1.2219	-1.1993	-1.1838	-1.2228
	10	-0.7613	-0.7451	-0.7333	-0.7150
	20	-0.8379	-0.8106	-0.7974	-0.7618
1965	1	-1.4082	-1.3979	-1.3831	-1.4124
	10	-0.9455	-0.9213	-0.9069	-0.8899
	20	-1.0784	-1.0427	-1.0276	-0.9896
1966	1	-0.6312	-0.6080	-0.5760	-0.6246
	10	-0.1622	-0.1347	-0.1143	-0.0815
	20	-0.3113	-0.2362	-0.2094	-0.1407
1967	1	-0.5077	-0.4958	-0.4786	-0.5077
	10	-0.0159	0.0013	0.0163	0.0416
	20	-0.1604	-0.0947	-0.0762	-0.0289
1968	1	-0.4024	-0.3775	-0.3423	-0.4074
	10	0.0859	0.1252	0.1555	0.2064
	20	-0.0529	0.0047	0.0373	0.1382

APPENDIX B. RMS TEMPERATURE ERROR (DEGREES C) VERSUS MODEL ΔZ AND TUNNING PARAMETERS P3 AND AM3

P3=3.5 AM3=2

	Winter			Spring		
	1	10	20	1	10	20
61	0.27	0.27	0.27	0.28	0.27	0.27
62	0.17	0.18	0.18	0.21	0.20	0.20
63	0.20	0.20	0.20	0.17	0.17	0.17
64	0.14	0.14	0.14	0.11	0.08	0.09
65	0.13	0.13	0.13	0.22	0.19	0.17
66	0.14	0.13	0.13	0.10	0.09	0.09
67	0.35	0.42	0.46	0.11	0.09	0.09
68	0.19	0.18	0.18	0.07	0.07	0.07
	Summer			Fall		
	1	10	20	1	10	20
61	0.63	0.61	0.59	0.21	0.22	0.24
62	0.74	0.71	0.69	0.44	0.50	0.54
63	0.65	0.66	0.68	0.24	0.33	0.26
64	0.66	0.58	0.61	0.33	0.42	0.48
65	0.72	0.64	0.60	0.45	0.54	0.44
66	0.72	0.72	0.71	0.08	0.09	0.10
67	0.72	0.70	0.63	0.16	0.19	0.21
68	0.65	0.63	0.63	0.17	0.17	0.17
	Year					
	1	10	20			
61	1.21	0.49	0.51			
62	0.43	0.95	0.67			
63	1.26	0.53	0.59			
64	1.15	0.48	0.50			
65	1.03	0.42	0.43			
66	0.54	0.58	0.52			
67	1.06	0.54	0.64			
68	0.98	0.45	0.41			

	P3=4.6	AM3=4.5				
	Winter			Spring		
	1	10	20	1	10	20
61	0.27	0.27	0.27	0.27	0.27	0.27
62	0.18	0.20	0.19	0.21	0.20	0.21
63	0.14	0.14	0.14	0.11	0.08	0.09
65	0.14	0.14	0.14	0.18	0.18	0.17
66	0.14	0.14	0.14	0.10	0.09	0.09
67	0.35	0.41	0.47	0.10	0.09	0.09
68	0.18	0.18	0.18	0.07	0.07	0.07
	Summer			Fall		
	1	10	20	1	10	20
61	0.63	0.62	0.59	0.20	0.22	0.24
62	0.74	0.72	0.69	0.42	0.47	0.54
63	0.67	0.67	0.69	0.22	0.32	0.30
64	0.67	0.59	0.59	0.26	0.39	0.48
65	0.72	0.65	0.61	0.38	0.48	0.38
66	0.73	0.72	0.73	0.09	0.09	0.10
67	0.70	0.69	0.65	0.16	0.19	0.21
68	0.65	0.64	0.64	0.17	0.17	0.17
	Year					
	1	10	20			
61	1.33	0.87	0.91			
62	0.53	0.43	0.39			
63	1.39	0.92	0.99			
64	1.24	0.82	0.90			
65	1.09	0.66	0.76			
66	0.68	0.35	0.36			
67	1.29	0.93	1.03			
68	1.09	0.66	0.70			

P3=7.5 AM3=5

	Winter			Spring		
	1	10	20	1	10	20
61	0.27	0.27	0.27	0.27	0.27	0.27
62	0.20	0.20	0.20	0.21	0.21	0.21
63	0.20	0.20	0.20	0.18	0.17	0.18
64	0.14	0.14	0.14	0.10	0.08	0.09
65	0.14	0.14	0.14	0.18	0.18	0.17
66	0.14	0.14	0.14	0.10	0.09	0.09
67	0.47	0.50	0.54	0.11	0.09	0.09
68	0.18	0.18	0.18	0.07	0.07	0.07
	Summer			Fall		
	1	10	20	1	10	20
61	0.62	0.61	0.58	0.22	0.25	0.25
62	0.73	0.72	0.68	0.50	0.55	0.59
63	0.66	0.66	0.68	0.27	0.37	0.27
64	0.65	0.59	0.60	0.38	0.50	0.54
65	0.70	0.64	0.60	0.46	0.56	0.43
66	0.72	0.71	0.71	0.09	0.11	0.11
67	0.69	0.69	0.62	0.18	0.21	0.22
68	0.64	0.63	0.63	0.17	0.17	0.17

	Year		
	1	10	20
61	0.85	0.51	0.50
62	0.54	0.79	0.72
63	0.89	0.59	0.66
64	0.77	0.44	0.44
65	0.65	0.40	0.42
66	0.49	0.67	0.64
67	0.89	0.65	0.71
68	0.75	0.57	0.60

P3=7.5 AM3=6

	Winter			Spring		
	1	10	20	1	10	20
61	0.27	0.27	0.27	0.27	0.27	0.27
62	0.20	0.20	0.20	0.21	0.21	0.21
63	0.20	0.20	0.20	0.18	0.18	0.18
64	0.14	0.14	0.14	0.10	0.08	0.09
65	0.14	0.14	0.14	0.18	0.18	0.16
66	0.14	0.14	0.14	0.10	0.09	0.09
67	0.48	0.50	0.54	0.10	0.09	0.09
68	0.18	0.18	0.18	0.07	0.07	0.07
	Summer			Fall		
	1	10	20	1	10	20
61	0.62	0.61	0.59	0.22	0.25	0.25
62	0.73	0.72	0.68	0.50	0.55	0.59
63	0.66	0.66	0.68	0.28	0.37	0.27
64	0.66	0.59	0.60	0.38	0.50	0.54
65	0.69	0.64	0.60	0.45	0.55	0.41
66	0.72	0.71	0.72	0.09	0.10	0.11
67	0.69	0.69	0.62	0.18	0.21	0.23
68	0.64	0.64	0.63	0.17	0.17	0.17

	Year		
	1	10	20
61	0.89	0.56	0.55
62	0.53	0.72	0.68
63	0.92	0.64	0.71
64	0.79	0.50	0.54
65	0.68	0.41	0.44
66	0.49	0.60	0.59
67	0.96	0.68	0.78
68	0.79	0.60	0.62

P3=7 AM3=7

	Winter			Spring		
	1	10	20	1	10	20
61	0.27	0.27	0.27	0.27	0.27	0.27
62	0.20	0.21	0.21	0.21	0.21	0.21
63	0.20	0.20	0.20	0.18	0.17	0.18
64	0.14	0.14	0.14	0.10	0.08	0.09
65	0.14	0.14	0.14	0.17	0.18	0.17
66	0.14	0.14	0.14	0.10	0.09	0.09
67	0.44	0.48	0.53	0.10	0.09	0.09
68	0.18	0.18	0.18	0.07	0.07	0.07
	Summer			Fall		
	1	10	20	1	10	20
61	0.62	0.61	0.59	0.22	0.24	0.25
62	0.73	0.72	0.69	0.47	0.53	0.58
63	0.66	0.66	0.69	0.26	0.37	0.28
64	0.66	0.59	0.59	0.35	0.48	0.53
65	0.70	0.65	0.61	0.42	0.52	0.39
66	0.73	0.72	0.72	0.09	0.10	0.11
67	0.69	0.69	0.63	0.18	0.21	0.23
68	0.64	0.64	0.63	0.17	0.17	0.17

	Year		
	1	10	20
61	1.01	0.66	0.70
62	0.49	0.59	0.57
63	1.01	0.81	0.82
64	0.90	0.58	0.71
65	0.78	0.46	0.56
66	0.51	0.47	0.45
67	1.05	0.84	0.87
68	0.85	0.61	0.67

	P3=8	AM3=4				
	Winter			Spring		
	1	10	20	1	10	20
61	0.27	0.27	0.27	0.27	0.27	0.27
62	0.20	0.20	0.20	0.21	0.21	0.21
63	0.20	0.20	0.20	0.18	0.17	0.18
64	0.14	0.14	0.14	0.11	0.08	0.09
65	0.14	0.14	0.14	0.19	0.18	0.17
66	0.14	0.14	0.14	0.09	0.09	0.09
67	0.50	0.51	0.54	0.11	0.09	0.09
68	0.18	0.18	0.18	0.07	0.07	0.07
	Summer			Fall		
	1	10	20	1	10	20
61	0.62	0.61	0.58	0.23	0.25	0.25
62	0.73	0.71	0.68	0.52	0.56	0.59
63	0.65	0.65	0.67	0.28	0.37	0.28
64	0.65	0.59	0.61	0.41	0.51	0.54
65	0.69	0.64	0.60	0.50	0.58	0.45
66	0.71	0.71	0.71	0.10	0.11	0.11
67	0.69	0.69	0.62	0.18	0.21	0.22
68	0.64	0.63	0.62	0.17	0.17	0.17
	Year					
	1	10	20			
61	0.73	0.43	0.48			
62	0.62	0.95	0.82			
63	0.80	0.54	0.58			
64	0.67	0.38	0.37			
65	0.56	0.43	0.49			
66	0.54	0.82	0.78			
67	0.85	0.65	0.65			
68	0.71	0.70	0.64			

	P3=8	AM3=5				
	Winter			Spring		
	1	10	20	1	10	20
61	0.27	0.27	0.27	0.27	0.27	0.27
62	0.20	0.20	0.20	0.21	0.21	0.21
63	0.20	0.20	0.20	0.18	0.17	0.18
64	0.14	0.14	0.14	0.10	0.08	0.09
65	0.14	0.14	0.14	0.19	0.18	0.17
66	0.14	0.14	0.14	0.10	0.09	0.09
67	0.50	0.51	0.54	0.11	0.09	0.09
68	0.18	0.18	0.18	0.07	0.07	0.07
	Summer			Fall		
	1	10	20	1	10	20
61	0.62	0.61	0.58	0.22	0.25	0.25
62	0.73	0.71	0.68	0.52	0.56	0.59
63	0.65	0.66	0.68	0.28	0.38	0.28
64	0.65	0.59	0.61	0.41	0.51	0.54
65	0.69	0.64	0.60	0.48	0.57	0.43
66	0.71	0.71	0.71	0.10	0.11	0.11
67	0.69	0.69	0.62	0.19	0.21	0.22
68	0.64	0.63	0.62	0.17	0.17	0.17
	Year					
	1	10	20			
61	0.77	0.45	0.47			
62	0.59	0.83	0.77			
63	0.82	0.55	0.61			
64	0.68	0.41	0.40			
65	0.57	0.42	0.45			
66	0.53	0.73	0.71			
67	0.86	0.64	0.67			
68	0.73	0.67	0.62			

LIST OF REFERENCES

Adamec, D., R. L. Elsberry, R. W. Garwood Jr., and R. L. Haney, 1981: An embedded mixed layer-ocean circulation model, Dyn. Atmos. Oceanogr., 6, 69-96.

De Szoeke, R.A. and P.B. Rhines, 1976: Asymptotic regimes in mixed-layer deepening, J. Mar. Res, 34, 111-116.

Ekman, V.A., 1905: On the influence of earth's rotation on ocean currents, Arkiv. Mat. Astron. Fysik., 2:1-53.

Garwood, R.W., 1977: An oceanic mixed layer model capable of simulating cyclic states, J. Phys. Oceanogr., 7, 455-468.

Large, W.G. and S. Pond, 1982: Sensible and latent heat flux measurements over the ocean, J. Phys. Oceanogr.,12, 464-482.

Niiler, P.P., 1975: Deepening of the wind-mixed layer, J. Mar. Res., 33, 405-422.

Oberhuber, J.M., 1993: Simulation of the Atlantic Circulation with a coupled sea ice-mixed layer-isopycnal general circulation model. Part I: Model description, J. Phys. Oceanogr., 23, 808-829.

Tabata, S., 1965: Variability of oceanographic conditions at Ocean Station "P" in the northeast Pacific Ocean, J. Fish. Res. Bd. Can., III series IV: June 1965, 367-418.

INITIAL DISTRIBUTION LIST

		No. Copies
1.	Defense Technical Information Center 8725 John J. Kingman Rd., STE 0944 Ft. Belvoir, VA 22060-6218	2
2.	Dudley Knox Library Naval Postgraduate School 411 Dyer Rd. Monterey, CA 93943-5101	2
3.	Chairman(Code OC/BF) Department of Oceanography Naval Postgraduate School Monterey, CA 93943-5101	1
4.	Prof. Roland W. Garwood Department of Oceanography Naval Postgraduate School Monterey, CA 93943-5101	1
5.	Ms. Arlene A. Guest Department of Oceanography Naval Postgraduate School Monterey, CA 93943-5101	1
6.	Office of Naval Research 800 North Quincy Street, Ballston Tower One Arlington, VA 22217-5660	1
7.	Office of Naval Research Code 3220M ATTN: Dr. Manual Fiadeiro 800 North Quincy Street Arlington, VA 22217-5660	1
8.	LT David M. Hone 314 Euclid Ave. Monterey, CA 93940	2